calculated positions were fixed for the final cycles refinement. The largest peaks of the final difference Fourier were situated close to the atoms of solvent molecules.

Acknowledgment. We thank the National Science Foundation for support. R.H.C. is a National Science Foundation Postdoctoral Fellow.

Registry No. Mo_4(OXA), 123358-63-4; W_4(OXA), 123380-77-8; Mo_4(PFT), 123358-64-5; W_4(PFT), 123358-65-6; W_4(FDC), 136301-48-9; Mo_4(DOQ), 136327-68-9; Mo_4(DAND), 123358-68-9; W_4(DAND), 123380-78-9; Mo_4(AND), 123358-66-7; W_4(AND), 123358-67-8; Mo_4(DON), 136301-49-0; Mo_4(OXA)$^+$, 136301-43-4; W_4(OXA)$^+$, 136301-45-6; Mo_4(PFT)$^+$, 136301-47-8; W_4(PFT)$^+$, 136327-67-8; $Mo_2(O_2C$-t-$Bu)_4$, 55946-68-4; $W_2(O_2C$-t-$Bu)_4$, 86728-84-9; $Mo_2(O_2C$-t-$Bu_2)(MeCN)_6(BF_4)_2$, 134078-47-0; $Mo_2(O_2C$-t-$Bu)_3(MeCN)_2(BF_4)$, 134078-49-2; $[Mo_2(O_2CH)_3]_2(\mu$-$O_2CCO_2)$, 136301-50-3; $[W_2(O_2CH)_3]_2(\mu$-$O_2CCO_2)$, 136301-51-4; $[W_2(O_2CH)_4]_2$, 136327-69-0; $[Mo_2H_6]_2(\mu$-2,7-$O_2N_2C_8H_4)^{6-}$, 136301-52-5; W, 7440-33-7; Mo, 7439-98-7; 1,1'-ferrocenedicarboxylic acid, 1293-87-4.

Supplementary Material Available: Tables of fractional coordinates and thermal parameters, anisotropic thermal parameters, and bond distances and bond angles and VERSORT drawings (11 pages); listings of F_o and F_c values (18 pages). Ordering information is given on any current masthead page.

Thermal and Photochemical Transformations of Organoiridium Phosphide Complexes. Mechanistic Studies on Carbon–Phosphorus Bond Formation To Generate Cyclometalated Hydride Complexes by α-Hydride Abstraction

Michael D. Fryzuk,*,† Kiran Joshi, Raj K. Chadha,§ and Steven J. Rettig‡

Contribution from the Department of Chemistry, University of British Columbia, 2036 Main Mall, Vancouver, BC, Canada V6T 1Z1. *Received April 23, 1991*

Abstract: The thermal and photolytic transformations of a series of methyliridium(III) phosphide complexes are described. Complexes of the formula $Ir(CH_3)PR_2[N(SiMe_2CH_2PPh_2)_2]$ (R = Ph, Me) rearrange thermally to generate the corresponding cyclometalated derivatives *fac*-$Ir(\eta^2$-$CH_2PR_2)H[N(SiMe_2CH_2PPh_2)_2]$; continued thermolysis results in the formation of the iridium(I) phosphine complexes $Ir(PMeR_2)[N(SiMe_2CH_2PPh_2)_2]$. Under photolytic conditions the phosphide derivatives rearrange directly to the phosphine complexes with no observable intermediates. The phenylphosphide complex $Ir(CH_3)PHPh[N(SiMe_2CH_2PPh_2)_2]$ rearranges directly to the phosphine derivative $Ir(PHPhMe)[N(SiMe_2CH_2PPh_2)_2]$ both thermally and photolytically with no observable intermediates. Crystals of $Ir(CH_3)PPh_2[N(SiMe_2CH_2PPh_2)_2]$ are monoclinic with a = 13.506 (3) Å, b = 13.665 (3) Å, c = 22.816 (7) Å, β = 92.35 (2)°, Z = 4, D_c = 1.454 g cm^{-3}, and space group $P2_1/c$. The structure was solved by the Patterson method and refined by full-matrix least-squares procedures to R = 0.034 and R_w = 0.037 for 3993 reflections with $I \geq 3\sigma(I)$. Crystals of *fac*-$Ir(\eta^2$-$CH_2PPh_2)H[N(SiMe_2CH_2PPh_2)_2]$ are monoclinic with a = 9.253 (2) Å, b = 21.950 (5) Å, c = 20.081 (4) Å, β = 90.74 (2)°, Z = 4, D_c = 1.50 g cm^{-3}, and space group $P2_1/c$. The structure was solved by conventional heavy-atom techniques and was refined in blocks (with the Ir atom in every cycle) by using least-squares procedures down to R = 0.0356 and R_w = 0.0370 for 4448 reflections with $I \geq 3\sigma(I)$. Mechanistic studies showed that the formation of the cyclometalated hydride does not involve reductive transfer of the methyl and the phosphide ligands to form a phosphine complex followed by intramolecular C–H bond activation, rather C–H bond abstraction occurs first followed then by C–P bond formation. Transition-state arguments are used to rationalize the difference in the reactivity of the phenylphosphide complex for which no cyclometalated intermediate was detected.

Introduction

Metal complexes mediate many complex transformations by virtue of the fact that the reacting moieties are proximate to one another (i.e., cis disposed) and under the influence of both the metal center and the ancillary ligands. The formation of C–C, C–H, and C–X bonds (X is a heteroatom, e.g., O, N, Si, P, etc.) within the coordination sphere of a metal complex is of both fundamental interest[1] and practical interest in the development of new reagents for organic synthesis.[2] Although a number of studies on the formation of C–X bonds have been made, in particular, formation of C–O[3] and C–N[4] functionalities, little has been reported on the formation of carbon–phosphorus bonds[5] (C–P) at a transition-metal center. Part of the reason for the dearth of results in this area is that there are very few metal complexes that contain both a hydrocarbyl ligand and a suitable phosphorus donor such as a phosphide (PR_2^-) to study *intramolecular* C–P bond formation.

Sometime ago, we reported[6] the preparation and some reaction studies[7] of a series of methyliridium phosphide complexes of the general formula $Ir(CH_3)PR_2[N(SiMe_2CH_2PPh_2)_2]$ (R = aryl). These complexes were subsequently shown[8] to rearrange to cy-

Scheme I

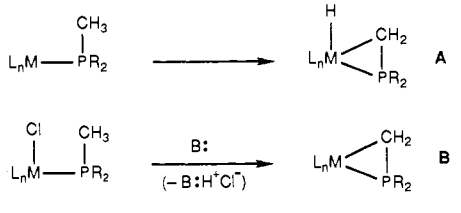

† E. W. R. Steacie Fellow (1990–92).

‡ Present address: Department of Chemistry, University of California at San Diego, La Jolla, CA 92093.

§ Professional Officer: UBC Crystallographic Service.

(1) Collman, J. P.; Hegedus, L. S.; Norton, J. R.; Finke, R. G. *Principles and Applications of Organotransition Metal Chemistry*; University Science Books: Mill Valley, CA, 1987; pp 669–937.

(2) (a) Posner, G., Ed. *Pure Appl. Chem.* **1988**, *60*, 1–144. (b) Hegedus, L. S. *J. Organomet. Chem.* **1988**, *342*, 147. (c) Parshall, G. W.; Nugent, W. A.; Chan, D. M. T.; Tam, W. *Pure Appl. Chem* **1985**, *57*, 1809. (d) Negishi, E. *Organometallics in Organic Synthesis*; Wiley: New York, NY, 1980.

(3) (a) Bernard, K. A.; Atwood, J. D. *Organometallics* **1989**, *8*, 795. (b) Komiya, S.; Akai, Y.; Tanaka, T.; Yamamoto, T.; Yamamoto, A. *Organometallics* **1985**, *4*, 1130.

(4) (a) Murahashi, S.-I.; Yoshimura, N.; Tsumiyama, T.; Kojima, T. *J. Am. Chem. Soc.* **1983**, *105*, 5002. (b) Fryzuk, M. D.; MacNeil, P. A.; Rettig, S. J. *J. Organomet. Chem.* **1987**, *332*, 345.

0002-7863/91/1513-8724$02.50/0

clometalated derivatives of the formula *fac*-Ir(η^2-CH_2PR_2)H[N-($SiMe_2CH_2PPh_2$)$_2$]; as this transformation involves the formation of a C–P bond, as well as the activation of a C–H bond, the process was examined in more detail.

Cyclometalation of a phosphine ligand is often the undesired result of attempts to perform intermolecular carbon–hydrogen bond activation with a coordinatively unsaturated phosphine-containing metal complex.[9] Cyclometalated phosphine ligands can also arise upon attempted reaction of strong bases with certain metal phosphine complexes that also have halide donors.[10] Both of these processes[11] are illustrated in Scheme I. What became apparent was that the formation of the cyclometalated derivatives *fac*-Ir(η^2-CH_2PR_2)H[N($SiMe_2CH_2PPh_2$)$_2$] did not arise via first reductive transfer of the methyl and the phosphide ligands to generate the corresponding phosphine complex, followed by a carbon–hydrogen bond oxidative addition (process A in Scheme I);[9] rather the cyclometalated derivatives are the kinetic products on the pathway to the formation of the thermodynamic iridium(I) phosphine complexes Ir($MePR_2$)[N($SiMe_2CH_2PPh_2$)$_2$]. In this paper are presented synthetic and mechanistic details of a new process for the formation of cyclometalated hydride complexes.

Experimental Section

General Procedures. All manipulations were performed under prepurified nitrogen in a Vacuum Atmospheres HE-553-2 workstation equipped with a MO-40-2H purification system or in Schlenk-type glassware. Toluene and hexanes were dried and deoxygenated by distillation from sodium benzophenone ketyl under argon. Tetrahydrofuran was predried by refluxing over CaH_2 and then distilled from sodium benzophenone ketyl under argon. Deuterated benzene (C_6D_6, 99.6 atom % D) and deuterated toluene (C_7D_8, 99.6 atom % D), purchased from MSD, were dried over activated 4-Å molecular sieves, vacuum transferred, and freeze–pumped–thawed three times before use.

The preparation of the methyl phosphide complex Ir(CH_3)PPh_2[N-($SiMe_2CH_2PPh_2$)$_2$] was as reported[6] previously; the deuterated derivative (Ir(CD_3)PPh_2[N($SiMe_2CH_2PPh_2$)$_2$] 99.8% deuterated by ^{1}H NMR spectroscopy) was prepared analogously from the corresponding deuteriomethyl iodide complex Ir(CD_3)I[N($SiMe_2CH_2PPh_2$)$_2$]. The reagents KOBu^t and PH_2Ph were purchased from Aldrich and used as received. Dimethylphoshine, ($HPMe_2$)[12] and benzyl potassium (KCH_2Ph)[13] were prepared according to the literature procedures. $KPMe_2$ was prepared by vacuum transfer of a slight excess of $HPMe_2$ to KCH_2Ph in THF; after removal of the volatiles the resulting solid was washed with hexanes, dried under vacuum, and used without further purification.

The ^{1}H NMR spectra were recorded in C_6D_6 or $CD_3C_6D_5$ on the Varian XL-300 or the Bruker WH-400 spectrometer. With C_6D_6 as the solvent, the spectra were referenced to the residual solvent protons at 7.15 ppm; when $CD_3C_6D_5$ was used, the spectra were referenced to the CD_2H residual proton at 2.09 ppm. The ^{31}P{^{1}H} NMR spectra were recorded at 121.421 MHz on the Varian XL-300 and were referenced to external $P(OMe)_3$ set at +141.00 ppm relative to 85% H_3PO_4. The ^{13}C{^{1}H} NMR and ^{2}H{^{1}H} NMR spectra were run in C_6D_6 at 75 and 40 MHz, respectively, on the Varian XL-300 spectrometer. The ^{13}C{^{1}H} NMR spectra were referenced at 128.00 ppm (triplet for the solvent), and the ^{2}H{^{1}H} spectra were referenced at 7.15 ppm, the residual solvent protons. Variable-temperature NMR spectral studies and various 1D- and 2D-NMR experiments (e.g. selective decoupling studies, APT and HETCOR experiments) were conducted on the Varian XL-300 spectrometer. Infrared spectra were recorded on a Pye-Unicam SP-1100 or a Nicolet 5DX Fourier transform spectrophotometer with the samples as KBr pellets or in solution between 0.1-mm NaCl plates. UV–vis spectra were recorded on a Perkin-Elmer 5523 UV–vis spectrophotometer stabilized at 20 °C. Carbon, hydrogen, and nitrogen analyses were performed by Mr. P. Borda of this department.

Ir(CH_3)PMe_2[N($SiMe_2CH_2PPh_2$)$_2$] (1b). Complex **1b** was prepared by adding a 2-mL toluene suspension of $KPMe_2$ (46 mg, 0.47 mmol) at −30 °C to the toluene solution (10 mL) of Ir(CH_3)I[N-($SiMe_2CH_2PPh_2$)$_2$] (400 mg, 0.46 mmol) also at −30 °C. The reaction was complete after 1 h as evidenced by the change of the green color of the reaction mixture to purple. Because complex **1b** is thermally unstable, it was prepared and characterized in situ only. ^{1}H NMR (300 MHz, C_7D_8, −30 °C): $SiMe_2$, −0.03 (s), 0.26 (s); PCH_2Si, 1.99, 2.12 (dt, $^2J_{gem}$ = 12.0 Hz, J_{app} = 4.9 Hz); Ir–CH_3, 1.26 (four-line pattern, $^3J_{P,H}$ = 4.0 Hz); PMe_2, 0.55 (d, $^3J_{P,H}$ = 6.7 Hz); PPh_2, 7.17 (m, para/meta), 7.75 (m, ortho). ^{31}P{^{1}H} NMR (C_7D_8, −30 °C): PMe_2, 94.30 (t, $^2J_{P,P}$ = 25.1 Hz); PPh_2, 25.11 (d, $^2J_{P,P}$ = 25.0 Hz).

Ir(CH_3)I(PH_2Ph)[N($SiMe_2CH_2PPh_2$)$_2$] (2). Preparation of **2** involved dropwise addition of a toluene solution (5 mL) of PH_2Ph (12 mg, 0.11 mmol) to a toluene solution (10 mL) of Ir(CH_3)I[N($SiMe_2CH_2PPh_2$)$_2$] (100 mg, 0.11 mmol) at room temperature. The reaction was instantaneous as the green color of the methyl iodide derivative changed to light yellow. The solution was stirred for an hour and concentrated to ~1 mL by pumping off the solvent under vacuum. Addition of ~1 mL of hexanes to the reaction mixture afforded light yellow crystals of **2** within a few hours. The product was washed with small amounts of hexanes (0.5 mL) and dried in vacuo. Yield: 90%. Anal. Calcd for $C_{37}H_{40}NP_3Si_2Ir$: C, 45.68; H, 4.13; N, 1.44. Found: C, 45.91; H, 4.30; N, 1.20. ^{1}H NMR (300 MHz, C_6D_6): $SiMe_2$, 0.39 (s), 0.42 (s); PCH_2Si, 1.60, 1.95 (dt, J_{gem} = 12.2 Hz, J_{app} = 4.5 Hz); Ir–CH_3, 1.51 (four-line pattern, $^3J_{P,H}$ = 4.7 Hz); P*H*Ph, 5.00 (dt, $^2J_{P,H}$ = 155.1 Hz, $^3J_{P,H}$ = 6.9 Hz); PPh_2, 7.00 (m, para/meta), 8.00, 8.17 (m, ortho). ^{31}P{^{1}H} NMR (C_6D_6): PPh_2, −20.78 (d, $^2J_{P,P}$ = 16.6 Hz); PH_2Ph, −84.57 (t, $^2J_{P,P}$ = 15.8 Hz). ^{13}C{^{1}H} NMR (C_6D_6): $SiMe_2$, 5.83 (s), 7.13 (s); PCH_2Si, 21.11 (br t); Ir–CH_3, −6.69 (dt, $^2J_{P,C(trans)}$ = 90.1 Hz, $^2J_{P,C(cis)}$ = 5.8 Hz; PPh_2, 128–136 (m).

Ir(CH_3)PHPh[N($SiMe_2CH_2PPh_2$)$_2$] (1c). Synthesis of **1c** was achieved by adding KOBu^t (12 mg, 0.10 mmol) to a toluene solution (10 mL) of Ir(CH_3)I(PH_2Ph)[N($SiMe_2CH_2PPh_2$)$_2$] (**2**, 100 mg, 0.10 mmol) at room temperature. The reaction proceeded within minutes as the light yellow solution of **2** changed to brick-red due to the formation of **1c**. The excess solvent was pumped off under vacuum. The residual powder was dissolved in hexanes (5 mL) and filtered through Celite in order to remove KI. The solution was concentrated to ~1 mL and stored at −30 °C for crystallization. The product was isolated as brick-red crystalline material which was washed with hexanes (0.5 mL) and dried in vacuo. Yield: 80%. Anal. Calcd for $C_{37}H_{45}NP_3Si_2Ir$: C, 52.59; H, 5.37; N, 1.66. Found: C, 52.97; H, 5.67; N, 1.49. ^{1}H NMR (300 MHz, C_7D_8): $SiMe_2$, −0.10 (s), 0.37 (s); PCH_2Si, 1.86 (br); Ir–CH_3, 1.19 (four-line pattern, $^3J_{P,H}$ = 4.0 Hz); P*H*Ph, 2.83 (dt, $^1J_{P,H}$ = 195.0 Hz, $^3J_{P,H}$ = 5.4 Hz); PPh_2, 6.81, 6.99, 7.10, 7.29 (m, para/meta), 7.35–7.90 (br, ortho). ^{31}P{^{1}H} NMR (C_6D_6): PHPh, 26.95 (t, $^2J_{P,P}$ = 16.8 Hz); PPh_2, 10.85 (d, $^2J_{P,P}$ = 16.9 Hz). UV–vis: $\lambda_{(max)}$(hexanes) = 462 nm, ϵ = 1820 mol^{-1} L cm^{-1}.

***fac*-Ir(η^2-CH_2PPh_2)H[N($SiMe_2CH_2PPh_2$)$_2$] (3a).** Ir(CH_3)PPh_2[N-($SiMe_2CH_2PPh_2$)$_2$] (**1a**, 150 mg, 0.16 mmol) was heated under N_2 in benzene (5 mL) in the dark (flask wrapped in aluminum foil) for 5 h in an oil bath set at 50 °C. The solvent was removed in vacuo and the resultant oil was crystallized from a hexanes–toluene mixture (1 mL) at room temperature. Light yellow crystals of the product were obtained within a few hours which were washed with hexanes (1 mL) and dried in vacuo. Yield: 82%. Anal. Calcd for $C_{43}H_{49}NP_3Si_2Ir$: C, 56.07; H, 5.36; N, 1.52. Found: C, 56.28; H, 5.42; N, 1.40. ^{1}H NMR (300 MHz, C_6D_6): $SiMe_2$, −0.78 (s), 0.65 (s), 0.68 (s), 0.81 (s); PCH_2Si, 1.40 (t, J_{app} = 13.7 Hz), 1.75 (t, J_{app} = 13.7 Hz), 2.10 (m), 2.49 (m); η^2-CH_2PPh_2, 1.32 (br, m), 2.00 (br, t); PPh_2, 6.60–7.25 (m, para/meta), 7.45–8.05 (m, ortho); Ir–H, −19.90 (td, $^2J_{P,H}$ = 16.7 Hz, $^2J_{P,H}$ = 9.9 Hz). ^{31}P{^{1}H} NMR (C_6D_6): CH_2PPh_2, 12.39 ($^2J_{PA,PX}$ = 32.0 Hz, $^2J_{PM,PX}$ = 5.5 Hz); CH_2PPh_2, 15.60 ($^2J_{PA,PM}$ = 298.2 Hz, $^2J_{PM,PX}$ = 6.4 Hz); η^2-CH_2PPh_2, −46.80 ($^2J_{PA,PM}$ = 297.9 Hz, $^2J_{PA,PX}$ = 30.4 Hz). ^{13}C{^{1}H} NMR (C_7D_8): $SiMe_2$, 4.91 (s), 5.62 (s), 5.81 (s), 7.00 (s); PCH_2Si,

(5) (a) Le Floch, P.; Marinetti, A.; Ricard, L.; Mathey, F. *J. Am. Chem. Soc.* **1990**, *112*, 2407. (b) Mathey, F. *Angew. Chem., Int. Ed. Engl.* **1987**, *26*, 275.
(6) Fryzuk, M. D.; Joshi, K. *Organometallics* **1989**, *8*, 722.
(7) Fryzuk, M. D.; Bhangu, K. *J. Am. Chem. Soc.* **1988**, *110*, 961.
(8) Fryzuk, M. D.; Joshi, K.; Chadha, R. K. *J. Am. Chem. Soc.* **1989**, *111*, 4498.
(9) (a) Shinomoto, R. S.; Desrosiers, P. J.; Harper, T. G. P.; Flood, T. C. *J. Am. Chem. Soc.* **1990**, *112*, 704. (b) Green, M. L. H.; Parkin, G.; Mingqin, C.; Prout, K. *J. Chem. Soc., Chem. Commun.* **1984**, 1400. (c) Rabinovich, D.; Parkin, G. *J. Am. Chem. Soc.* **1990**, *112*, 5381. (d) Desrosiers, P. J.; Shinomoto, R. S.; Flood, T. C. *J. Am. Chem. Soc.* **1986**, *108*, 7964. (e) Werner, H.; Gotzig, J. *Organometallics* **1983**, *2*, 547. (f) Harris, T. V.; Rathke, J. W.; Muetterties, E. L. *J. Am. Chem. Soc.* **1978**, *100*, 6966.
(10) (a) Mainz, V.; Andersen, R. A. *Organometallics* **1984**, *3*, 675. (b) Bryndza, H. E.; Fong, L. K.; Paciello, R. C.; Tam, W.; Bercaw, J. E. *J. Am. Chem. Soc.* **1987**, *109*, 1444. (c) Al-Jibori, S.; Crocker, C.; McDonald, W. S.; Shaw, B. L. *J. Chem. Soc., Dalton Trans.* **1981**, 1572.
(11) One can also generate the M(η^2-CH_2PR_2) unit by reaction of the lithio reagents $LiCH_2PR_2$ with metal halides, see: (a) Karsch, H. H.; Schmidbaur, H. *Z. Naturforsch.* **1977**, *B32*, 762. (b) Karsch, H. H.; Deubelly, B.; Hofmann, J.; Pieper, U.; Muller, G. *J. Am. Chem. Soc.* **1988**, *110*, 3654. (c) Schore, N. E.; Young, S. J.; Olmstead, M. M.; Hofmann, P. *Organometallics* **1983**, *2*, 1769.
(12) Parshall, G. W. *Inorg. Synth.* **1968**, *11*, 157.
(13) Schlosser, M.; Hartmann, J. *Angew. Chem., Int. Ed. Engl.* **1973**, *12*, 508.

23.25 (d, $^1J_{C,P}$ = 12.3 Hz), 28.90 (d, $^1J_{C,P}$ = 21.5 Hz); Ir–CH_2P, –21.62 (m); PPh_2, 127–136 (m). UV-vis: $\lambda_{(max)}$(toluene) = 360 nm, ϵ = 5425 mol^{-1} L cm^{-1}. The deuterated analogue, *fac*-Ir(η^2-CD_2PPh_2)D[N-($SiMe_2CH_2PPh_2$)$_2$] (d_3-**3a**) was prepared as above with Ir(CD_3)PPh_2-[N($SiMe_2CH_2PPh_2$)$_2$] (d_3-**1a**).

***fac*-Ir(η^2-CH_2PMe_2)H[N($SiMe_2CH_2PPh_2$)$_2$] (3b).** Warming the freshly prepared toluene solution (10 mL) of Ir(CH_3)PMe_2[N-($SiMe_2CH_2PPh_2$)$_2$] (**1b**) from –30 °C to room temperature resulted in the formation of **3b** within 5 min. The solution was stirred for an hour. After this time, the solvent was pumped off under vacuum. The residual light yellow powder was dissolved in toluene (1 mL) and filtered through Celite in order to remove KI generated during the preparation of **1b**. The solution was concentrated to 0.5 mL and left for crystallization at room temperature. Light yellow crystals of **3b** were obtained overnight. Yield: 78% (calculated from the amount of the methyl iodide starting material used and its 100% conversion to **3b**). Anal. Calcd for $C_{33}H_{45}NP_3Si_2Ir$: C, 49.75; H, 5.65; N, 1.77. Found: C, 49.67; H, 5.86; N, 1.66. ^{1}H NMR (300 MHz, C_6D_6): $SiMe_2$, 0.10 (s), 0.51 (s), 0.76 (s), 0.85 (s); PCH_2Si, 1.40 (t, J_{app} = 11.2 Hz), 1.71 (t, J_{app} = 11.2 Hz), 2.18 (m), 2.51 (m); η^2-CH_2PMe_2, 1.30 (br, m), 2.07 (br); PMe_2, 1.40, 1.75 (m), 2.39 (s), PPh_2, 6.70–8.15 (m); Ir–H, –20.10 (td, $^2J_{P,H}$ = 16.8 Hz, $^2J_{P,H}$ = 8.5 Hz). ^{31}P{^{1}H} NMR (C_6D_6): CH_2PPh_2, 12.19 ($^2J_{PA,PX}$ = 39.2 Hz, $^2J_{PM,PX}$ = 12.2 Hz); CH_2PPh_2, 14.14 ($^2J_{PA,PM}$ = 300.9 Hz, $^2J_{PM,PX}$ = 12.0 Hz); η^2-CH_2PMe_2, –68.15 ($^2J_{PA,PM}$ = 301.1 Hz, $^2J_{PA,PX}$ = 39.7 Hz).

Ir(PCH_3R_2)[N($SiMe_2CH_2PPh_2$)$_2$] (4a: R = Ph; 4b: R = Me). Method I: Thermolysis, General Procedure. Complexes **4a** and **4b** were synthesized by heating a benzene or toluene solution (5 mL) of **3a** and **3b**, respectively, in a reaction vessel sealed under nitrogen for 24 h at 100 °C. During this time, the light yellow colored solutions of the species **3a** and **3b** changed to orange. The excess solvent was pumped off under vacuum and the resultant orange oils were crystallized from hexanes at room temperature.

Ir(PCH_3Ph_2)[N($SiMe_2CH_2PPh_2$)$_2$] (4a). Starting material: *fac*-Ir-(η^2-CH_2PPh_2)H[N($SiMe_2CH_2PPh_2$)$_2$] (**3a**, 100 mg, 0.11 mmol). Yield: 85%. Anal. Calcd for $C_{43}H_{49}NP_3Si_2Ir$: C, 56.07; H, 5.36; N, 1.52. Found: C, 55.80; H, 5.35; N, 1.40. ^{1}H NMR (400 MHz, C_6D_6): $SiMe_2$, 0.20 (s); PCH_2Si, 1.91 (t, J_{app} = 5.2 Hz); PCH_3Ph_2, 1.38 (d, $^3J_{P,H}$ = 7.5 Hz); PPh_2, 6.90–7.10 (m, para/meta), 7.53, 7.62 (m, ortho). ^{31}P{^{1}H} NMR (C_6D_6): PPh_2, 25.30 (d, $^2J_{P,P}$ = 22.8 Hz); PCH_3Ph_2, –1.79 (t, $^2J_{P,P}$ = 22.3 Hz). UV-vis: $\lambda_{(max)}$(toluene) = 388 nm, ϵ = 2130 mol^{-1} L cm^{-1}.

Ir(PMe_3)[N($SiMe_2CH_2PPh_2$)$_2$] (4b). Starting material: *fac*-Ir(η^2-CH_2PMe_2)H[N($SiMe_2CH_2PPh_2$)$_2$] (**3b**, 100 mg, 0.13 mmol). Yield: 80%. Anal. Calcd for $C_{33}H_{45}NP_3Si_2Ir$: C, 49.75; H, 5.65; N, 1.77. Found: C, 49.74; H, 5.70; N, 1.71. ^{1}H NMR (300 MHz, C_6D_6): $SiMe_2$, 0.20 (s); PCH_2Si, 1.88 (t, J_{app} = 5.0 Hz); PMe_3, 0.85 (d, $^3J_{P,H}$ = 7.5 Hz); PPh_2, 7.15 (m, para/meta), 8.11 (m, ortho). ^{31}P{^{1}H} NMR (C_6D_6): PPh_2, 21.51 (d, $^2J_{P,P}$ = 25.2 Hz); PMe_3, –59.54 (t, $^2J_{P,P}$ = 25.2 Hz).

Method II: Photolysis, General Procedure. The preparation of phosphine complex **4a** involved the photolysis, using a 140-W Hg lamp, of diphenylphosphide complex **2a** in a benzene solution (5 mL) at room temperature for 24 h. Because dimethylphosphide complex **2b** was unstable above –30 °C, its photolysis was carried out at –30 °C with a N_2 laser in order to produce **4b**. This transformation took approximately 3 h. The workup of the final orange solutions of **4a** and **4b** was the same as described above in method I.

Ir(PCH_3Ph_2)[N($SiMe_2CH_2PPh_2$)$_2$] (4a). Starting material: Ir-(CH_3)PPh_2[N($SiMe_2CH_2PPh_2$)$_2$] (**1a**, 50 mg, 0.05 mmol). Yield: 78%.

Ir(PMe_3)[N($SiMe_2CH_2PPh_2$)$_2$] (4b). Starting material: Ir(CH_3)-PMe_2[N($SiMe_2CH_2PPh_2$)$_2$] (**2b**, 50 mg, 0.06 mmol). Yield: 85%.

Ir($PHCH_3Ph$)[N($SiMe_2CH_2PPh_2$)$_2$] (4c). Complex **4c** was prepared by heating a benzene, toluene, or hexanes solution (5 mL) of phosphide complex **1c** (100 mg, 0.10 mmol) at 60 °C for an hour or by photolyzing (140-W Hg lamp) its benzene solution (5 mL) for 18 h at room temperature. The original brick-red solution turned orange as the transformation proceeded. The reaction mixtures were worked up in the usual manner which involved the removal of the solvent in vacuo and crystallization of the orange oil at room temperature. The isolated yields of **4c** are similar from both routes (~85%). Anal. Calcd for $C_{37}H_{45}NP_3Si_2Ir$: C, 52.59; H, 5.37; N, 1.66. Found: C, 52.39; H, 5.30; N, 1.65. ^{1}H NMR (300 MHz, C_6D_6): $SiMe_2$, 0.26 (s), 0.28 (s); PCH_2Si, 1.93 (m); PCH_3HPh, 1.07 (dd, $^3J_{P,H}$ = 7.9 Hz, $^3J_{H,H}$ = 3.8 Hz); PCH_3HPh, 5.00 (dm, $^1J_{P,H}$ = 140 Hz); PPh_2, 6.90–7.40 (m, para/meta), 7.90 (m, ortho). ^{31}P{^{1}H} NMR (C_6D_6): PPh_2, 22.60 (d, $^2J_{P,P}$ = 18.3 Hz); PHPh, –39.61 (t, $^2J_{P,P}$ = 18.1 Hz). UV-vis: $\lambda_{(max)}$(hexanes) = 390 nm, ϵ = 3000 mol^{-1} L cm^{-1}.

Ir(=CH_2)[N($SiMe_2CH_2PPh_2$)$_2$] + PHR_2 (R = Ph, Bu^t) Reactions. General Procedure. A toluene solution (10 mL) of Ir(=CH_2)[N-($SiMe_2CH_2PPh_2$)$_2$] (**5**) was cooled to –78 °C in a dry ice–ethanol bath for 15 min. To it was added a 1-mL toluene solution containing PHR_2. The original purple color of **5** turned wine red immediately. This wine red colored compound was characterized as Ir(=CH_2)(PHR_2)[N-($SiMe_2CH_2PPh_2$)$_2$] (**6**); characterization of these complexes was performed by ^{1}H and ^{31}P{^{1}H} NMR spectroscopy at –78 °C. Warming a solution of **6** to –30 °C resulted in the formation of *fac*-Ir(η^2-CH_2PR_2)H[N($SiMe_2CH_2PPh_2$)$_2$] (**7**) in which the cyclometalated phosphorus is trans to the amide donor. The solution was stirred for 10 min at room temperature and then the solvent was removed in vacuo. The yellow oil was dissolved in toluene (1 mL) from which pale yellow crystals of **7** were isolated within an hour. The toluene solution of **7** was stirred under an inert atmosphere for 48 h at room temperature which resulted in its conversion to the isomeric *fac*-Ir(η^2-CH_2PR_2)H[N-($SiMe_2CH_2PPh_2$)$_2$] (**8**) having the hydride ligand trans to the amide donor. The solution was pumped to dryness under vacuum and worked up as described above for the individual complexes.

Ir(=CH_2)($PHPh_2$)[N($SiMe_2CH_2PPh_2$)$_2$] (6a). Starting material: Ir(=CH_2)[N($SiMe_2CH_2PPh_2$)$_2$] (**5**, 100 mg, 0.14 mmol); $PHPh_2$ (21 mg, 0.15 mmol). ^{1}H NMR (300 MHz, C_7D_8, –78 °C): $SiMe_2$, 0.09 (s), 0.81 (s); PCH_2Si, 1.75 (br); Ir=CH_2, 12.08 (four-line pattern, $^3J_{P,H}$ = 14.4 Hz); $PHPh_2$, 5.90 (other half obscured by the phenyl resonances); PPh_2, 6.70–7.40 (m, para/meta), 8.45 (m, ortho). ^{31}P{^{1}H} NMR (C_7D_8): CH_2PPh_2, 13.45 (s); $PHPh_2$, 3.90 (s).

***fac*-Ir(η^2-CH_2PPh_2)H[N($SiMe_2CH_2PPh_2$)$_2$] (7a).** Starting material: Ir(=CH_2)[N($SiMe_2CH_2PPh_2$)$_2$] (**5**, 100 mg, 0.14 mmol); $PHPh_2$ (21 mg, 0.15 mmol). Yield: 85%. Anal. Calcd for $C_{43}H_{49}NP_3Si_2Ir$: C, 56.07; H, 5.36; N, 1.52. Found: C, 56.53; H, 5.52; N, 1.50. ^{1}H NMR (400 MHz, C_6D_6): $SiMe_2$, 0.52 (s), 0.71 (s), 0.76 (s), 0.82 (s); PCH_2Si, 1.36 (m), 1.40 (m), 1.60 (t, J_{app} = 9.0 Hz), 2.25 (m); η^2-CH_2PPh_2, 1.25 (br, m), 1.58 (m); PPh_2, 6.50–7.49 (m, para/meta), 7.90–8.45 (m, ortho); Ir–H, –11.88 (dddd, $^2J_{P,H(trans)}$ = 133.3 Hz, $^2J_{P,H(cis)}$ = 19.8 Hz, $^2J_{P,H(cis)}$ = 11.8 Hz). ^{31}P{^{1}H} NMR (C_7D_8): CH_2PPh_2, –16.17 (br t, $^2J_{P,P}$ = 12.6 Hz); CH_2PPh_2, 13.44 ($^2J_{PA,PM}$ = 310.1 Hz, $^2J_{PM,PX}$ = 10.3 Hz); η^2-CH_2PPh_2, –58.20 ($^2J_{PA,PM}$ = 310.8 Hz, $^2J_{PA,PX}$ = 10.3 Hz). ^{13}C{^{1}H} NMR (C_7D_8): $SiMe_2$, 3.18 (s), 3.59 (s), 3.73 (s), 7.13 (s); PCH_2Si, 14.38 (br s), 23.08 (br s); Ir–CH_2P, –38.20 (br); PPh_2, 127–136 (m). UV-vis: $\lambda_{(max)}$(toluene) = 360 nm, ϵ = 2205 mol^{-1} L cm^{-1}.

***fac*-Ir(η^2-CH_2PPh_2)H[N($SiMe_2CH_2PPh_2$)$_2$] (3a).** Starting material: *fac*-Ir(η^2-CH_2PPh_2)H[N($SiMe_2CH_2PPh_2$)$_2$] (**7a**, 75 mg, 0.08 mmol). Yield: 80%. The spectroscopic data and elemental analysis of this complex are given above.

Ir(=CH_2)($PHBu^t_2$)[N($SiMe_2CH_2PPh_2$)$_2$] (6d). Starting material: Ir(=CH_2)[N($SiMe_2CH_2PPh_2$)$_2$] (**5**, 100 mg, 0.14 mmol); $PHBu^t_2$ (17 mg, 0.15 mmol). ^{1}H NMR (300 MHz, C_7D_8, –78 °C): $SiMe_2$, 0.70 (s), 0.74 (s); PCH_2Si, 2.30 (br); PBu^t_2, 1.10 (s), 1.15 (s); Ir=CH_2, 16.26 (four-line pattern, $^3J_{P,H}$ = 18.0 Hz); $PHBu^t_2$, 3.36 (br, d, $^1J_{P,H}$ = 216.0 Hz); PPh_2, 6.40–8.15 (m). ^{31}P{^{1}H} NMR (C_7D_8): CH_2PPh_2, 17.85 (s); $PHBu^t_2$, 18.71 (s).

***fac*-Ir(η^2-$CH_2PBu^t_2$)H[N($SiMe_2CH_2PPh_2$)$_2$] (7d).** Starting material: Ir(=CH_2)[N($SiMe_2CH_2PPh_2$)$_2$] (**5**, 100 mg, 0.14 mmol); $PHBu^t_2$ (17 mg, 0.15 mmol). Yield: 78%. Anal. Calcd for $C_{39}H_{57}NP_3Si_2Ir$: C, 53.16; H, 6.52; N, 1.59. Found: C, 53.71; H, 6.61; N, 1.70. ^{1}H NMR (300 MHz, C_7D_8): $SiMe_2$, 0.58 (s), 0.70 (s), 0.85 (s), 0.90 (s); PCH_2Si, 1.49 (m), 1.54 (m), 1.78 (m), 2.46 (m); η^2-$CH_2PBu^t_2$, 1.28 (br, m), 1.67 (m); PBu^t_2, 1.07 (s), 1.09 (s), 1.12 (s), 1.14 (s); PPh_2, 6.70–7.85 (m); Ir–H, –14.34 (dt, $^2J_{P,H(trans)}$ = 100.1 Hz, $^2J_{P,H(cis)}$ = 15.5 Hz). ^{31}P{^{1}H} NMR (C_6D_6): CH_2PPh_2, –17.73 ($^2J_{PA,PX}$ = 15.9 Hz, $^2J_{PM,PX}$ = 14.2 Hz); CH_2PPh_2, 4.55 ($^2J_{PA,PM}$ = 217.9 Hz, $^2J_{PM,PX}$ = 14.7 Hz); η^2-$CH_2PBu^t_2$, –23.74 ($^2J_{PA,PM}$ = 323.6 Hz, $^2J_{PA,PX}$ = 15.8 Hz). ^{13}C{^{1}H} NMR (C_7D_8): $SiMe_2$, 3.28 (s), 3.84 (s), 3.98 (s), 7.29 (s); PCH_2Si, 18.10 (d, $^2J_{P,C}$ = 13.7 Hz), 25.58 (s); Ir–CH_2P, –38.05 (br); PBu^t_2, 29.54 (s), 31.67 (s); PPh_2, 128–134 (m).

***fac*-Ir(η^2-$CH_2PBu^t_2$)H[N($SiMe_2CH_2PPh_2$)$_2$] (3d).** Starting material: *fac*-Ir(η^2-$CH_2PBu^t_2$)H[N($SiMe_2CH_2PPh_2$)$_2$] (**7d**, 50 mg, 0.06 mmol). Yield: 86%. Anal. Calcd for $C_{39}H_{57}NP_3Si_2Ir$: C, 53.16; H, 6.52; N, 1.59. Found: C, 53.32; H, 6.43; N, 1.50. ^{1}H NMR (300 MHz, C_7D_8): $SiMe_2$, 0.65 (s), 0.82 (s), 0.96 (s), 1.14 (s); PCH_2Si, 2.15 (m), 2.35 (m), 2.71 (m); η^2-$CH_2PBu^t_2$, 1.28 (br, m), 1.67 (m); PBu^t_2, 1.50 (s), 1.62 (s), 1.68 (s), 1.74 (s); PPh_2, 6.90–8.42 (m); Ir–H, –21.62 (dt, $^2J_{P,H(trans)}$ = 84.0 Hz, $^2J_{P,H(cis)}$ = 36.0 Hz). ^{31}P{^{1}H} NMR (C_7D_8): CH_2PPh_2, 16.53 ($^2J_{PA,PX}$ = 32.8 Hz, $^2J_{PM,PX}$ = 4.9 Hz); CH_2PPh_2, 18.74 ($^2J_{PA,PM}$ = 289.8 Hz, $^2J_{PM,PX}$ = 5.5 Hz); η^2-$CH_2PBu^t_2$, 3.50 ($^2J_{PA,PM}$ = 289.2 Hz, $^2J_{PA,PX}$ = 32.9 Hz). ^{13}C{^{1}H} NMR (C_7D_8): $SiMe_2$, 6.43 (s), 6.58 (s), 7.58 (s), 11.07 (s); PCH_2Si, 22.64 (d, $^2J_{P,C}$ = 11.9 Hz), 27.56 (d, $^2J_{P,C}$ = 21.9 Hz); Ir–CH_2P, –23.00 (br); PBu^t_2, 32.10 (s), 32.28 (s); PPh_2, 125–136 (m).

***fac*-Ir(η^2-CH_2PHPh)H[N($SiMe_2CH_2PPh_2$)$_2$] (7c).** A solution of Ir-(=CH_2)[N($SiMe_2CH_2PPh_2$)$_2$] (**5**, 150 mg, 0.27 mmol) in toluene (10 mL) was cooled to –78 °C in a dry ice–ethanol bath for 15 min. To it was added 1 mL of a toluene solution of PH_2Ph (23 mg, 0.21 mmol). The original purple color of **5** turned light yellow immediately. The solution was warmed to room temperature and stirred for an hour. The solvent was removed under vacuum, and the residue was recrystallized

from a hexanes–toluene mixture (0.5 mL) at room temperature. Yield: 75%. Anal. Calcd for $C_{37}H_{45}NP_3Si_2Ir$: C, 52.59; H, 5.37; N, 1.66. Found: C, 52.07; H, 5.54; N, 1.70. ^1H NMR (300 MHz, C_6D_6): $SiMe_2$, −0.05 (s), −0.20 (s), −0.35 (s), −0.69 (s); PCH_2Si, 1.95 (m), 2.10 (m); η^2-CH_2PHPh, 1.51 (m), 2.75 (br, m); P*H*Ph, 3.86 (d of d of m); PPh_2, 6.70–7.40 (m, para/meta), 7.50–7.90 (m, ortho); Ir–H, −12.87 (dt, $^2J_{P,H(trans)}$ = 149.3 Hz, $^2J_{P,H(cis)}$ = 19.1 Hz). $^{31}P\{^1H\}$ NMR (C_6D_6): CH_2PPh_2, 5.50 (m); CH_2PPh_2, −64.21 (m); η^2-CH_2PHPh, −93.25 (t, $^2J_{P,P}$ = 9.1 Hz).

***fac*-Ir(η^2-CHPhPMe$_2$)H[N(SiMe$_2$CH$_2$PPh$_2$)$_2$] (10).** Addition of a 2-mL toluene suspension of $KPMe_2$ (10 mg, 0.09 mmol) to a toluene solution (10 mL) of $Ir(CH_2Ph)Br[N(SiMe_2CH_2PPh_2)_2]$[14] (75 mg, 0.08 mmol) at room temperature resulted in a gradual change of color from the green color of the benzyl bromide complex to yellow. After this time, the solvent was removed in vacuo. The residue was dissolved in toluene (1 mL) and filtered through Celite in order to remove KBr. Recrystallization from toluene–hexanes (1 mL) afforded yellow crystals. Yield: 85%. Anal. Calcd for $C_{39}H_{49}NP_3Si_2Ir$: C, 53.65; H, 5.66; N, 1.60. Found: C, 53.43; H, 5.80; N, 1.68. ^1H NMR (300 MHz, C_6D_6): $SiMe_2$, 0.17 (s), 0.51 (s), 0.86 (s), 0.95 (s); PCH_2Si, 1.30 (m), 1.59 (m), 1.97 (m); η^2-C*H*PhPMe$_2$, 2.09 (m); PMe_2, 0.35 (d), 1.20 (d, $^3J_{P,H}$ = 15.0 Hz); PPh_2, 6.70–7.75 (m, para/meta), 8.80 (m, ortho); Ir–H, −10.82 (ddd, $^2J_{P,H(trans)}$ = 153.0 Hz, $^2J_{P,H(cis)}$ = 20.1 Hz, $^2J_{P,H(cis)}$ = 9.0 Hz). $^{31}P\{^1H\}$ NMR (C_6D_6): CH_2PPh_2, −7.39 (four-line pattern, $^2J_{P,P}$ = 9.5 Hz); CH_2PPh_2, −2.60 (four-line pattern, $^2J_{P,P}$ = 9.5 Hz, $^2J_{P,P}$ = 9.3 Hz); η^2-CHPhPMe$_2$, −11.19 (t, $^2J_{P,P}$ = 9.0 Hz).

Ir(PMe$_2$CH$_2$Ph)[N(SiMe$_2$CH$_2$PPh$_2$)$_2$] (11). Iridium(I) complex **11** was synthesized by stirring a toluene solution (5 mL) of **10** (50 mg, 0.06 mmol) for 2 weeks at room temperature (or 48 h at 80 °C) under a N_2 atmosphere. During this time, the light yellow colored solutions of **10** darkened to orange. The excess solvent was pumped off under vacuum and the resultant orange oil was recrystallized from hexanes at room temperature. Yield: 80%. Anal. Calcd for $C_{39}H_{49}NP_3Si_2Ir$: C, 53.65; H, 5.66; N, 1.60. Found: C, 53.53; H, 5.72; N, 1.50. ^1H NMR (300 MHz, C_6D_6): $SiMe_2$, 0.28 (s); PCH_2Si, 1.99 (t, J_{app} = 6.0 Hz); PCH_2PhMe$_2$, 2.55 (d, $^2J_{P,H}$ = 14.5 Hz); PCH_2PhMe_2, 0.83 (d, $^2J_{P,H}$ = 11.5 Hz); PPh_2, 7.21 (m, para/meta), 8.15 (m, ortho). $^{31}P\{^1H\}$ NMR (C_6D_6): CH_2PPh_2, 20.23 ($^2J_{P,P}$ = 23.8 Hz); CH_2PhPMe_2, −39.73 ($^2J_{P,P}$ = 23.8 Hz).

Ir(η^1-CH$_2$PPh$_2$)H(CO)[N(SiMe$_2$CH$_2$PPh$_2$)$_2$] (8a). A toluene solution (10 mL) of *fac*-Ir(η^2-CH_2PPh_2)H[N(SiMe$_2$CH$_2$PPh$_2$)$_2$] (**3a** or **7a**, 100 mg, 0.11 mmol) was loaded in a thick-walled reactor bomb equipped with a 5-mm Kontes needle valve. The vessel was attached to a vacuum line and degassed. The solution was exposed to excess CO gas (1 atm) and stirred for 48 h at room temperature. Toluene was removed in vacuo and the faint yellow residual powder was recrystallized from a toluene–hexanes mixture (1 mL). Yield: 90%. Anal. Calcd for $C_{44}H_{49}NOP_3Si_2Ir$: C, 55.68; H, 5.20; N, 1.48. Found: C, 55.42; H, 5.36; N, 1.60. ^1H NMR (400 MHz, C_6D_6): $SiMe_2$, 0.20 (s), 0.31 (s); PCH_2Si, 2.10 (dt, J_{gem} = 13.3 Hz, J_{app} = 6.6 Hz); η^1-CH_2PPh_2, 1.48 (br); PPh_2, 7.15 (m, para/meta), 7.79, 8.00 (m, ortho); Ir–H, −6.50 (td, $^2J_{P,H}$ = 18.0 Hz, $^3J_{P,H}$ = 9.0 Hz). $^{31}P\{^1H\}$ NMR (C_6D_6): $SiCH_2PPh_2$, 5.84 (d, $^3J_{P,P}$ = 11.9 Hz); $IrCH_2PPh_2$, 10.51 (t, $^3J_{P,P}$ = 11.6 Hz). $^{13}C\{^1H\}$ NMR (C_6D_6): $SiMe_2$, 2.81 (s), 3.22 (s); PCH_2Si, 32.15 (m); Ir–CO, 179.88 (dt, $^2J_{P,C}$ = 11.0 Hz, $^3J_{P,C}$ = 5.9 Hz); PPh_2, 124–138 (m). IR (toluene): $\nu_{(CO)}$ = 1961 cm^{-1} (vs), $\nu_{(Ir-H)}$ = 2095 cm^{-1} (m).

***fac*-Ir(CH$_3$)(η^2-CH$_2$PPh$_2$)[N(SiMe$_2$CH$_2$PPh$_2$)$_2$].** This complex was prepared by adding a toluene solution of $LiCH_2PPh_2$·TMEDA (40 mg, 0.13 mmol) to the toluene solution (10 mL) of $Ir(CH_3)I[N(SiMe_2CH_2PPh_2)_2]$ (100 mg, 0.11 mmol) at room temperature. The reaction took about an hour to go to completion as the green color of the methyl iodide complex changed to yellow. The excess solvent was removed in vacuo. The residue was dissolved in toluene (1 mL) and filtered through Celite in order to remove LiI. Several attempts were made to purify the product, but decomposition resulted upon attempts to recrystallize at room temperature under a N_2 atmosphere. ^1H NMR (300 MHz, C_6D_6): $SiMe_2$, −0.50 (s), 0.11 (s), 0.39 (s), 0.51 (s); PCH_2Si, 2.62 (m), 2.41 (m), 2.10 (m), 1.65 (m); Ir–CH_3, 1.89 (br); PPh_2, 6.54–7.24 (m, para/meta), 8.12 (m, ortho). $^{31}P\{^1H\}$ NMR (C_6D_6): CH_2PPh_2, 2.11 ($^2J_{PA,PX}$ = 35.2 Hz, $^2J_{PM,PX}$ = 5.1 Hz); CH_2PPh_2, 8.59 ($^2J_{PA,PM}$ = 326.3 Hz, $^2J_{PM,PX}$ = 6.0 Hz); η^2-CH_2PPh_2, −51.23 ($^2J_{PA,PM}$ = 337.8 Hz, $^2J_{PA,PX}$ = 36.4 Hz).

Kinetics of the Thermolysis Experiments. In a typical experiment, a stock solution of known concentration was prepared in the indicated solvent. Five-milliliter aliquots of the solution were placed in a solvent reservoir fused to a 1-cm optical cell equipped with a Kontes needle valve. During the thermolysis of the light-sensitive phosphide complexes, aluminum foil was wrapped around the vessel. The sample was thermolyzed in a temperature-controlled oil bath; the disappearance (or appearance in some cases) of the appropriate absorption band was followed with time using a Perkin-Elmer 5523 UV–vis spectrophotometer stabilized at 20 °C. Treatment of the data is described in the text.

Table I. Crystallographic Data

	1a	**3a**
compd	$Ir(CH_3)PPh_2[N(SiMe_2CH_2PPh_2)_2]$	$Ir(\eta^2$-$CH_2PPh_2)H[N(SiMe_2CH_2PPh_2)_2]$
formula	$C_{43}H_{49}IrNP_3Si_2$	$C_{43}H_{49}IrNP_3Si_2$
fw	921.2	921.2
cryst system	monoclinic	monoclinic
space group	$P2_1/c$	$P2_1/c$
a, Å	13.506 (3)	9.253 (2)
b, Å	13.665 (3)	21.950 (2)
c, Å	22.816 (7)	20.081 (4)
β, deg	92.35 (2)	90.74 (2)
V, Å^3	4207 (2)	4078 (1)
Z	4	4
$F(000)$	1856	1856
T, °C	21	20 ± 1
ρ_c, g/cm^3	1.45	1.50
diffractometer	Rigaku AFC6	Nicolet R3
λ, Å	0.71069	0.71069
μ(Mo Kα) cm^{-1}	33.59	33.27
2θ angle$_{max}$, deg	55.0	48
transmission factors	0.641–1.000	0.883–0.959
scan speed, deg/min	16 (up to 8 rescans)	variable, 3.91–14.65
data collected	$+h,+k,\pm l$	$+h,+k,\pm l$
total no. of reflcns	10071	7299
no. of unique data ($I \geq 3\sigma(I)$)	3993	4448
no. of parameters	451	238, 226 (see text)
$R(F_o)$	0.034	0.0356
$R_w(F_o)$	0.037	0.0370
shift$_{max}$ in final cycle	0.05	0.10
large peak, e/Å^3 (final diff map)	1.25	1.1

X-ray Crystallographic Analyses. Ir(CH$_3$)PPh$_2$[N(SiMe$_2$CH$_2$PPh$_2$)$_2$] (1a). Crystallographic data appear in Table I. The final unit-cell parameters were obtained by least-squares calculations on the setting angles for 25 reflections with 2θ = 14.0–20.9°. The intensities of three standard reflections, measured every 150 reflections throughout the data collection, remained essentially constant. The data were processed[15] and corrected for Lorentz and polarization effects and absorption (empirical, based on azimuthal scans for three reflections). A total of 10488 reflections with $2\theta \leq 55°$ was collected on a Rigaku AFC6S diffractometer, 10071 were unique (R_{int} = 0.048) and those 3993 having $I \geq 3\sigma(I)$ were employed in the solution and refinement of the structure.

The structure was solved by conventional heavy atom methods, the coordinates of the Ir, P, and Si atoms being determined from the Patterson function and those of the remaining non-hydrogen atoms from a subsequent difference Fourier synthesis. The non-hydrogen atoms were refined with anisotropic thermal parameters. Hydrogen atoms were fixed in idealized positions (C–H = 0.98 Å, $B_H = 1.2B_{bonded\ atom}$). Neutral atom scattering factors and anomalous dispersion corrections for all atoms were taken from the *International Tables for X-ray Crystallography*.[16] The function minimized was $\sum w(|F_o| - |F_c|)^2$ where $w = 4F_o^2/\sigma^2(F_o^2)$, $\sigma^2(F^2) = [S^2(C + 4B) + (0.04F^2)^2]/Lp^2$ (S = scan speed, C = scan count, B = normalized background count), $R = \sum||F_o| - |F_c||/\sum|F_o|$, $R_w = (\sum w(|F_o| - |F_c|)^2/\sum w|F_o|^2)^{1/2}$, and gof = $[\sum(|F_o| - |F_c|)^2/(m - n)]^{1/2}$. The largest residual peak (1.25 e Å^{-3}) was located 0.97 Å from the Ir atom. Selected bond lengths and selected bond angles are given in Tables II and III, respectively. Final atomic coordinates and equivalent isotropic thermal parameters are contained in Table S1 in supplementary material.

***fac*-Ir(η^2-CH$_2$PPh$_2$)H[N(SiMe$_2$CH$_2$PPh$_2$)$_2$] (3a).** A single crystal of **3a** was sealed in a Lindemann capillary and mounted along the largest

(14) Fryzuk, M. D.; MacNeil, P. A.; Massey, R. L.; Ball, R. G. *J. Organomet. Chem.* **1989**, *368*, 231.

(15) TEXSAN/TEXRAY structure analysis package which includes versions of the following: DIRDIF, direct methods for difference structures, by P. T. Beurskens; ORFLS, full-matrix least-squares, and ORFFE, function and errors, by W. R. Busing, K. O. Martin, and H. A. Levy; ORTEP II, illustrations, by C. K. Joh...so...

(16) *International Tables for X-Ray Crystallography*; Kynoch Press: Birmingham, U.K. (present distributor D. Reidel: Dordrecht, The Netherlands), 1974; Vol. IV, pp 99–102 and 149.

Table II. Bond Lengths (Å) with Estimated Standard Deviations in Parentheses

		$Ir(CH_3)PPh_2[N(SiMe_2CH_2PPh_2)_2]$ (**1a**)			
Ir–C(43)	2.126 (9)	P(1)–C(1)	1.808 (9)	Si(1)–N	1.714 (7)
Ir–P(1)	2.309 (2)	P(1)–C(7)	1.831 (8)	Si(1)–C(3)	1.86 (1)
Ir–P(2)	2.312 (2)	P(1)–C(13)	1.84 (1)	Si(1)–C(4)	1.89 (1)
Ir–P(3)	2.297 (2)	P(2)–C(2)	1.807 (9)	Si(1)–C(1)	1.91 (1)
Ir–C(43)	2.126 (9)	P(2)–C(25)	1.818 (8)	Si(2)–N	1.729 (8)
Ir–N	2.126 (6)	P(2)–C(19)	1.824 (9)	Si(2)–C(6)	1.85 (1)
		P(3)–C(31)	1.80 (1)	Si(2)–C(5)	1.85 (1)
		P(3)–C(37)	1.834 (9)	Si(2)–C(2)	1.87 (1)
		fac-$Ir(\eta^2\text{-}CH_2PPh_2)H[N(SiMe_2CH_2PPh_2)_2]$ (**3a**)			
Ir–P(1)	2.241 (2)	P(1)–C(1)	1.760 (8)	Si(1)–N	1.695 (6)
Ir–P(2)	2.272 (2)	P(1)–C(11)	1.828 (7)	Si(1)–C(2)	1.897 (7)
Ir–P(3)	2.291 (2)	P(1)–C(21)	1.817 (8)	Si(1)–C(4)	1.871 (8)
Ir–C(1)	2.203 (7)	P(2)–C(31)	1.833 (7)	Si(1)–C(5)	1.885 (9)
Ir–N	2.277 (6)	P(2)–C(41)	1.831 (7)	Si(2)–N	1.684 (6)
Ir–H	1.51 (6)	P(3)–C(3)	1.824 (8)	Si(2)–C(3)	1.927 (7)
		P(3)–C(51)	1.847 (7)	Si(2)–C(6)	1.882 (9)
		P(3)–C(61)	1.816 (7)	Si(2)–C(7)	1.87 (1)

Table III. Bond Angles (deg) with Estimated Standard Deviations in Parentheses

	$Ir(CH_3)PPh_2[N(SiMe_2CH_2PPh_2)_2]$ (**1a**)		
C(43)–Ir–N	159.0 (3)	Ir–N–Si(2)	118.9 (4)
C(43)–Ir–P(3)	87.4 (2)	Si(1)–N–Si(2)	121.8 (4)
C(43)–Ir–P(1)	91.2 (2)	C(1)–P(1)–C(13)	106.4 (5)
C(43)–Ir–P(2)	90.3 (2)	Ir–P(1)–C(1)	108.8 (3)
N–Ir–P(3)	113.2 (2)	C(1)–P(1)–C(7)	100.9 (5)
N–Ir–P(1)	87.4 (2)	Ir–P(1)–C(7)	111.7 (3)
N–Ir–P(2)	86.5 (2)	C(2)–P(2)–C(19)	104.2 (4)
P(3)–Ir–P(1)	105.35 (9)	Ir–P(2)–C(2)	105.3 (3)
P(3)–Ir–P(2)	87.95 (8)	C(2)–P(2)–C(25)	108.8 (4)
P(1)–Ir–P(2)	166.68 (8)	Ir–P(3)–C(31)	108.4 (3)
N–Si(1)–C(3)	113.6 (5)	Ir–P(3)–C(37)	117.7 (3)
N–Si(1)–C(4)	115.6 (4)	C(31)–P(2)–C(37)	100.3 (4)
N–Si(1)–C(1)	105.9 (4)	N–Si(2)–C(3)	105.2 (3)
C(3)–Si(1)–C(4)	107.8 (5)	N–Si(2)–C(6)	118.0 (4)
C(3)–Si(1)–C(1)	109.1 (5)	N–Si(2)–C(7)	116.5 (4)
C(4)–Si(1)–C(1)	104.3 (5)	P(1)–C(1)–Si(1)	106.3 (5)
Ir–N–Si(1)	119.2 (4)	P(2)–C(2)–Si(2)	107.1 (5)
	fac-$Ir(\eta^2\text{-}CH_2PPh_2)H[N(SiMe_2CH_2PPh_2)_2]$ (**3a**)		
C(1)–Ir–N	97.6 (3)	P(1)–Ir–H	70 (3)
C(1)–Ir–H	87 (3)	P(2)–Ir–H	83 (3)
C(1)–Ir–P(1)	46.7 (2)	P(3)–Ir–H	112 (3)
C(1)–Ir–P(2)	157.5 (2)	N–Ir–H	167 (3)
C(1)–Ir–P(3)	97.9 (2)	Ir–P(1)–C(11)	123.9 (2)
N–Ir–P(1)	103.8 (2)	C(1)–P(1)–C(11)	114.6 (3)
N–Ir–P(2)	88.4 (2)	Ir–P(1)–C(21)	127.4 (3)
N–Ir–P(3)	79.7 (1)	Ir–P(2)–C(2)	109.5 (2)
P(1)–Ir–P(2)	110.9 (1)	Ir–P(3)–C(3)	106.8 (2)
P(1)–Ir–P(3)	144.5 (1)	Ir–P(3)–C(51)	117.3 (2)
P(2)–Ir–P(3)	104.5 (1)	Ir–P(3)–C(61)	120.4 (2)
N–Si(1)–C(2)	106.5 (3)	Ir–C(1)–P(1)	67.8 (2)
N–Si(1)–C(5)	117.6 (4)	Ir–P(1)–C(1)	65.5 (2)
C(2)–Si(1)–C(5)	103.3 (4)	C(1)–P(1)–C(22)	114.0 (4)
C(4)–Si(1)–C(5)	103.8 (4)	C(21)–P(1)–C(11)	104.5 (4)
N–Si(2)–C(3)	105.2 (3)	Ir–N–Si(1)	113.4 (3)
N–Si(2)–C(6)	118.0 (4)	Ir–N–Si(2)	114.1 (1)
N–Si(2)–C(7)	116.5 (4)	Si(1)–N–Si(2)	131.0 (4)

dimension, and the cell parameters were obtained from 15 strong reflections with $15° < 2\theta < 30°$. Data were collected on a Nicolet R3 diffractometer following the procedure described previously.[17] The intensity of three monitor reflections measured after 100 reflections did not change significantly (3%) during data collection which took 132 h. The data were corrected for Lorentz and polarization effects. An empirical absorption correction that uses ψ scans was applied to the data based on an absorption profile averaged from five reflections with χ values near 90°. Details of the X-ray data collection are given in Table I.

Systematic absences ($h0l$, $l = 2n + 1$; $0k0$, $k = 2n + 1$) uniquely defined the $P2_1/c$ space group. The position of iridium was located from a sharpened Patterson synthesis and the remaining atoms were found on subsequent difference Fourier maps, using SHELX 1976. The structure was refined anisotropically in blocks during the least-squares calculations, with the Ir atom in every cycle, P, Si, N, H, and C(1) to C(26) (238 variables) in alternate cycles with C(41) to C(46) (226 variables). The hydrogen atom bonded to Ir was refined isotropically, and other hydrogen atoms were included at idealized positions (C–H = 0.95 Å) with isotropic U's set at 0.01 Å greater than the corresponding carbon atoms. Refinement minimizing the function $\sum w(|F_o| - |F_c|)^2$, where $w = 4F_o^2/\sigma^2(F_o^2)$, converged at $R = 0.0356$ and $R_w = 0.0370$. In the final cycles a weighting scheme of the form $w = 1/[\sigma^2(F) + pF^2]$ was employed with a final p value of 0.0012. No evidence of secondary extinction was found. The highest peak in the final difference Fourier map was 1.1 e Å^{-3}.

Computation was carried out on the University of Manitoba Computer Services Department's Amdahl 580/5850 mainframe computer. Sources of scattering factors and computer programs have been previously described.[17] The atomic coordinates for nonhydrogen atoms are given in Table S2 (supplementary material), and important bond distances and bond angles are given in Tables II and III, respectively.

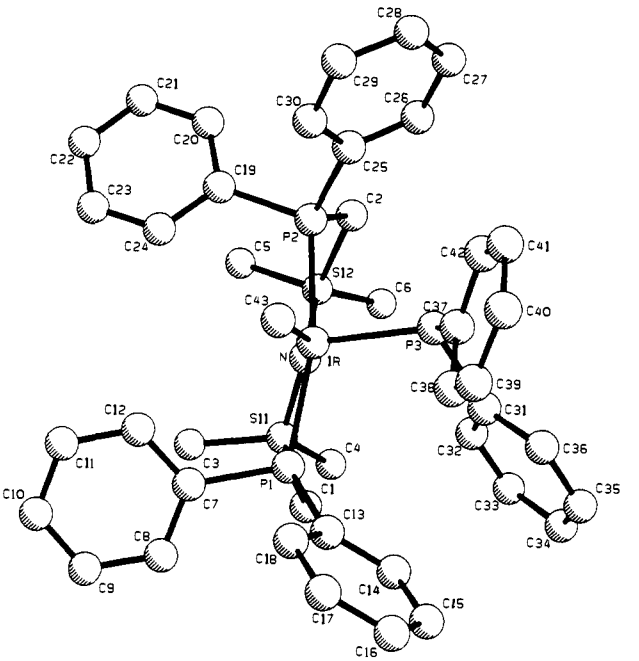

Figure 1. X-ray structure of $Ir(CH_3)PPh_2[N(SiMe_2CH_2PPh_2)_2]$ (**1a**).

Results and Discussion

X-ray Structure of $Ir(CH_3)PPh_2[N(SiMe_2CH_2PPh_2)_2]$. Earlier work from our laboratory concluded that the stereochemistry of $Ir(CH_3)PPh_2[N(SiMe_2CH_2PPh_2)_2]$ (**1a**) was square pyramidal with the methyl ligand occupying the apical position. This was based on nOe difference spectroscopy by comparison to other similar five-coordinate derivatives.[14,18] However, this has been found not to be in agreement with the results of a recent X-ray crystal structure determination.

Diffraction quality crystals of methyl diphenylphosphide complex **1a** were finally obtained after many earlier unsuccessful attempts. Some pertinent bond lengths and bond angles are listed in Tables II and III, respectively. Figure 1 shows that the overall geometry at the iridium center is best described as a distorted square pyramid with the methyl group in the basal plane and the diphenylphosphido group apical. The tridentate hybrid ligand is arranged in a quasimeridional fashion (P(1)–Ir–P(2) = 166.68 (8)°). The angle between the methyl carbon and the phosphide phosphorus atom (C(43)–Ir–P(3) = 87.4 (2)°) is close to the expected 90° angle for a square-pyramidal geometry. However, the angle between the phosphide group and the amide ligand (N–Ir–P(3) = 113.2 (2)°) is greater by ~23° from the expected 90° for an apical phosphide. The magnitude of Ir–P(3)–C(31) (108.4 (3)°) and Ir–P(3)–C(37) (117.7 (3)°) indicates that the geometry at the phosphorus in the PPh_2 ligand is pyrmidal. In-

(17) Chadha, R. K.; Drake, J. E.; Sarkar, A. B. *Inorg. Chem.* **1986**, *25*, 2201.

(18) Fryzuk, M. D.; MacNeil, P. A.; Ball, R. G. *J. Am. Chem. Soc.* **1986**, *108*, 6414.

Scheme II

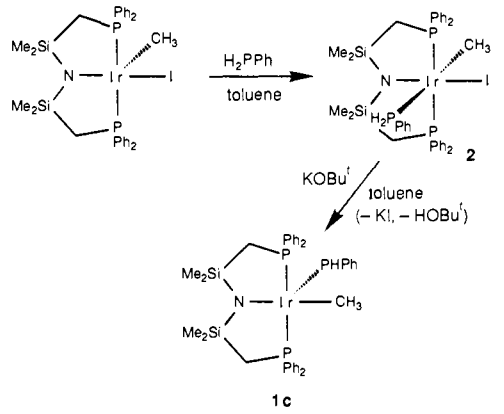

terestingly, the iridium lies above the square-pyramidal basal plane as evidenced by the angle between the methyl and the amide nitrogen: C(43)–Ir–N = 159.0 (3)°.

The solution data have now been reinterpreted in terms of the solid-state structure. The nOe difference experiment conducted on a benzene solution of **1a** shows a small enhancement of the methyl (Ir–CH_3) resonance upon irradiation of one of the two sets of methylene proton (PCH_2Si) resonances. No enhancement of the methyl proton resonance was observed upon irradiation of the other set of methylene signals. Our initial conclusion was that this was due to an apical methyl ligand; however, the enhancement was much smaller than that observed for the analogous experiment with the square-pyramidal species $Ir(CH_3)Br[N(SiMe_2CH_2PPh_2)_2]$ in which the methyl is apical.[19] On the basis of solid-state results the small nuclear Overhauser enhancement may be due to the methyl group lying below the basal plane in the distorted square pyramid.

Although the solid-state geometry for **1a** is a distorted square pyramid, for simplicity this molecule will be drawn as an undistorted square pyramid with the methyl ligand trans to the amide center and the phosphide ligand in the apical position.[20]

Synthetic Considerations. The preparation of phosphide alkyl derivatives **1** follows that of earlier work (eq 1).[6] Dimethyl-

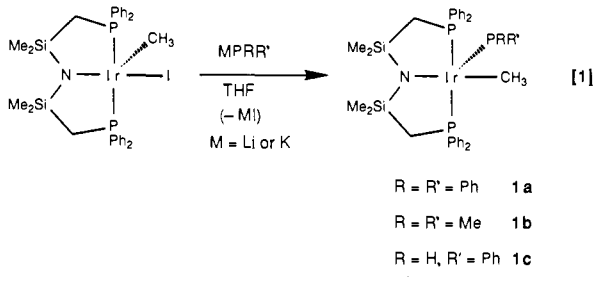

[1]

R = R' = Ph 1a

R = R' = Me 1b

R = H, R' = Ph 1c

phosphide complex **1b** is very thermally labile and therefore could not be isolated. It was prepared at −30 °C and characterized only spectroscopically at low temperatures.

In the case of the phenylphosphide derivative $Ir(CH_3)PHPh[N(SiMe_2CH_2PPh_2)_2]$ (**1c**), preparation by the route in eq 1 using freshly prepared in situ LiPHPh or even $Mg(PHPh)_2$·TMEDA generally led to impure mixtures. Along with the formation of the desired iridium(III) phenylphosphide complex, **1c**, there was a competitive reaction with trace free phenylphosphine with the starting methyl iodide complex to generate the octahedral phenylphosphine adduct $Ir(CH_3)I(PH_2Ph)[N(SiMe_2CH_2PPh_2)_2]$ (**2**). The free PH_2Ph may have arisen from the slow hydrolysis of the

Scheme III

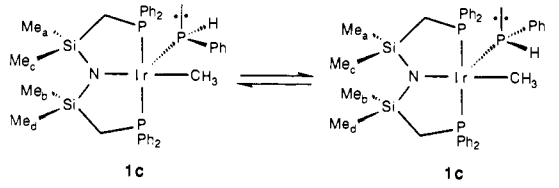

lithium or magnesium phenylphosphide reagents. A more efficient procedure was developed by deprotonation of the aforementioned octahedral iridium(III) phenylphosphine complex **2** with potassium *tert*-butoxide, $KOBu^t$ (Scheme II). The reaction proceeds within minutes at room temperature as the yellow color of the octahedral phosphine complex changes to a brick-red color. Phenylphosphide complex **1c** was isolated as brick-red crystals from hexanes at −30 °C in good yield (80%). The synthesis of complex **1c** was also attempted by the abstraction of HI from **2** with the base 1,8-diazabicyclo[5.4.0]undec-7-ene (DBU), but no reaction was observed.

The complex $Ir(CH_3)PHPh[N(SiMe_2CH_2PPh_2)_2]$ (**1c**) exhibits simple ^1H and $^{31}P\{^1H\}$ NMR spectra. The ^1H NMR spectrum consists of a sharp singlet at 0.37 ppm and a broad peak at −0.10 ppm for the silyl methyl protons at room temperature. As the temperature of the solution is lowered, the peak at −0.10 ppm broadens further and then splits into two singlets which are observed at −0.05 and 0.14 ppm (T_c = 280 K, $\Delta G^{\ddagger}$ = 58 ± 4 kJ mol^{-1}). In addition, the broad methylene resonance (2.00 ppm) and the phenyl resonance (7.80 ppm) split into multiplets. The different orientations of the substituents on the chiral phosphide ligand with respect to the tridentate ligand protons on the same side of the phosphide may result in different environments for those particular ligand protons (for example, the silyl methyls marked Me_a and Me_b in Scheme III). The silyl methyl protons on the side opposite to the phosphide ligand (labeled Me_c and Me_d in Scheme III) remain relatively unaffected by the different orientations of the apical phosphide ligand, and therefore, only a single coincidental resonance is observed. Presumably, the chiral, pyramidal phosphide ligand undergoes inversion through a planar intermediate that has overall C_s symmetry. In the complexes $CpRe(PHPh)NO(PPh_3)$[21] and $CpFe(PHPh)\{1,2\text{-}C_6H_4(PMePh)_2\}$,[22] the inversion barriers reported for the pyramidal phenylphosphide ligand are 48 and 60 kJ mol^{-1}, respectively. Thus, the activation barrier of 58 kJ mol^{-1} for the phosphide inversion mechanism in **1c** seems reasonable.

Thermolysis Reactions. Diphenylphosphide complex $Ir(CH_3)PPh_2[N(SiMe_2CH_2PPh_2)_2]$ (**1a**) is quite stable thermally in the solid state and can be stored at room temperature for months under an inert atmosphere without any noticeable decomposition. However, when thermolyzed in hydrocarbon solvents, typically benzene, toluene, or hexanes (50 °C in the dark for about 5 h), complex **1a** converts cleanly and quantitatively to the cyclometalated hydride species $fac\text{-}Ir(\eta^2\text{-}CH_2PPh_2)H[N(SiMe_2CH_2PPh_2)_2]$ (**3a**) (eq 2).

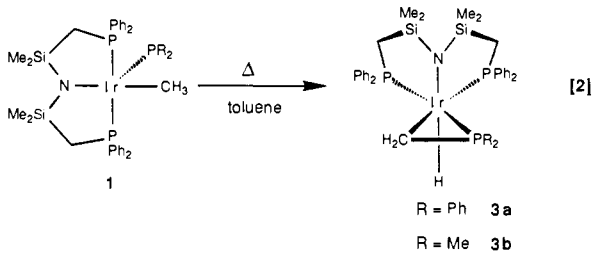

[2]

R = Ph 3a

R = Me 3b

Dimethylphosphide complex $Ir(CH_3)PMe_2[N(SiMe_2CH_2PPh_2)_2]$ (**1b**) is less stable than **1a** and, as mentioned before, has been prepared only in situ at −30 °C. When the sample

(19) Fryzuk, M. D.; MacNeil, P. A.; Rettig, S. J. *Organometallics* **1986**, *5*, 2469.

(20) As a referee has pointed out the stereochemistry of the five-coordinate iridium phosphide–methyl complex has undergone a quasiinversion with the methyl group now in a basal site as compared to the original apical position of the starting material. The origin of this stereochemical change is not clear since the tridentate ancillary ligand plays an important role in determining the final geometry of these species.[18]

(21) Buhro, W. E.; Gladysz, J. A. *Inorg. Chem.* **1985**, *24*, 3505.

(22) Crisp, G. T.; Salem, G.; Wild, S. B. *Organometallics* **1989**, *8*, 2360.

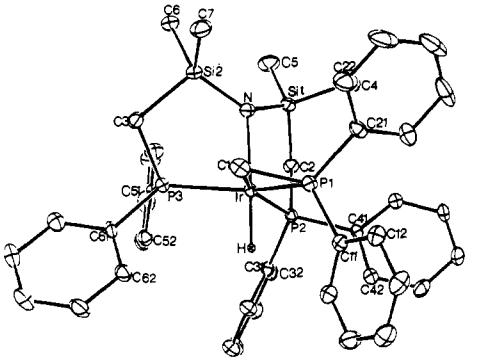

Figure 2. X-ray structure of $Ir(CH_2PPh_2)H[N(SiMe_2CH_2PPh_2)_2]$ (**3a**).

was warmed from −30 °C to room temperature, it cleanly converted to the cyclometalated hydride derivative *fac*-$Ir(\eta^2\text{-}CH_2PMe_2)H[N(SiMe_2CH_2PPh_2)_2]$ (**3b**). Complexes **3a** and **3b** were isolated in >80% yield as pale yellow crystalline solids which were stable under an inert atmosphere for months at room temperature. These complexes have been characterized by various NMR spectra techniques and single-crystal X-ray diffraction (for $\eta^2\text{-}CH_2PPh_2$ complex **3a**).

The ^1H and $^{31}P\{^1H\}$ NMR spectra of complex **3a** will serve to illustrate the typical spectral behavior of these complexes. In the ^1H NMR spectrum, four singlet resonances at −0.22, 0.65, 0.68, and 0.81 ppm are observed for the silyl methyl groups in the tridentate ligand backbone. Both pairs of methylene protons of the hybrid ligand backbone display four sets of resonances at 1.40 (t, J_{app} = 13.7 Hz), 1.75 (t, J_{app} = 13.7 Hz), 2.10 (m), and 2.49 ppm (m). The CH_2 protons of the $\eta^2\text{-}CH_2PPh_2$ moiety are observed as two diastereotopic multiplets at 1.32 (br) and 2.00 ppm (br, t). The hydride ligand trans to the amide resonates at −19.90 ppm (td, $^2J_{P,H}$ = 16.7 Hz, $^2J_{P,H}$ = 9.9 Hz). Hydride chemical shift values are related to the trans influence order (CO > P > N) of the ligand positioned trans to the hydride.[23] In octahedral complexes containing the hybrid tridentate ligand,[24] a hydride trans to the amide center typically resonates at −19 to −25 ppm; however, when it is trans to a phosphine, the chemical shift range is −9 to −12 ppm. The hydride trans to a carbonyl moiety is normally observed between −6 and −7 ppm.

The $^{31}P\{^1H\}$ NMR spectrum of **3a** shows an AMX pattern for this molecule, indicating that all three phosphorus centers are nonequivalent. Two of the phosphorus nuclei are strongly coupled to each other, but weakly coupled to the third. The chemical shifts of the phosphorus nuclei belonging to the tridentate ligand [12.39 ppm (dd, $^2J_{PA,PX}$ = 32.0 Hz, $^2J_{PM,PX}$ = 5.5 Hz) and 15.60 ppm (dd, $^2J_{PA,PM}$ = 298.2 Hz, $^2J_{PM,PX}$ = 6.4 Hz)] are well within the expected range; however, the resonance of the phosphorus nucleus in the $\eta^2\text{-}CH_2PPh_2$ moiety is shifted upfield (−46.80 ppm, dd, $^2J_{PA,PM}$ = 297.9 Hz, $^2J_{PA,PX}$ = 30.4 Hz), a phenomenon that has been observed before in other metallacyclic structures.[25]

X-ray Structure of *fac*-$Ir(\eta^2\text{-}CH_2PPh_2)H[N(SiMe_2CH_2PPh_2)_2]$ (3a). The X-ray crystal structure of **3a** is shown in Figure 2. Selected bond lengths and bond angles are listed in Tables II and III, respectively. The structure reveals that the ancillary tridentate ligand has isomerized to the facial coordination mode (P(2)–Ir–P(3) = 104.5°) with the hydride ligand trans to the amide donor; the $\eta^2\text{-}CH_2PPh_2$ moiety occupies the remaining cis sites of the distorted octahedron. The distortions from true octahedral geometry in the molecule are not unexpected given the steric demands of the tridentate ligand and the $\eta^2\text{-}CH_2PPh_2$ metallacyclic ring. The Ir–P(1) bond length (2.241 (2) Å) in the three-membered ring is 0.03 and 0.05 Å shorter than the other two Ir–P bond lengths (2.272 (2) and 2.292 (2) Å) of the hybrid tridentate ligand. In the related complex $IrCl_2(\eta^2\text{-}CH_2PMePh)(PMe_2Ph)_2$, the parameters reported for the metallacycle are very similar.[10c]

Further Thermolysis of the Cyclometalated Complexes. The cyclometalated derivatives are stable indefinitely in the solid state; however, in solution they gradually rearrange to generate the simple iridium(I) phosphine complexes **4a** (R = Ph) and **4b** (R = Me), as summarized in eq 3. The reaction is extremely slow even at 50 °C; heating toluene solutions of **3a** or **3b** to 100 °C for 24 h is generally the technique utilized.

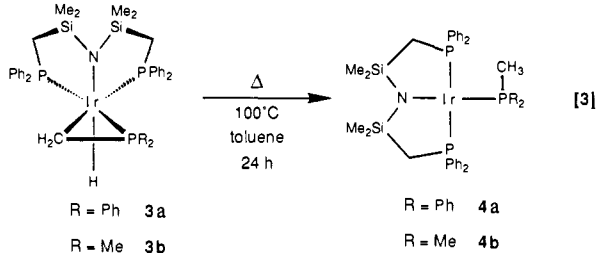

Photolysis Reactions. Upon photolysis of methyl phosphide complexes **1a** and **1b**, iridium(I) phosphine complexes **4a** and **4b**, respectively, are produced directly (eq 4). Diphenylphosphide

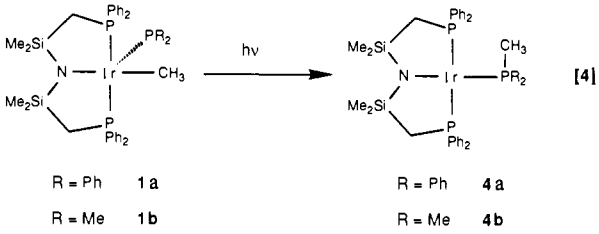

complex **1a** was photolyzed for 24 h in benzene solution at room temperature with a 140-W Hg lamp; however, due to the thermal sensitivity of dimethylphosphide derivative **1b**, its photolysis was carried out at −30 °C in toluene with a N_2 laser. Attempts to detect any intermediates were unsuccessful; monitoring these reactions over a period of time indicated only the presence of the starting methyl phosphide and the final iridium(I) phosphine derivative.

Thermolysis and Photolysis of $Ir(CH_3)PHPh[N(SiMe_2CH_2PPh_2)_2]$ (1c). The behavior of phenylphosphide complex **1c** upon thermolysis contrasts that of the other phosphide complexes **1a** and **1b**. Heating a benzene solution of **1c** for 1 h results in the formation of the iridium(I) phosphine complex $Ir(PHPhMe)[N(SiMe_2CH_2PPh_2)_2]$ (**4c**) (eq 5). The corre-

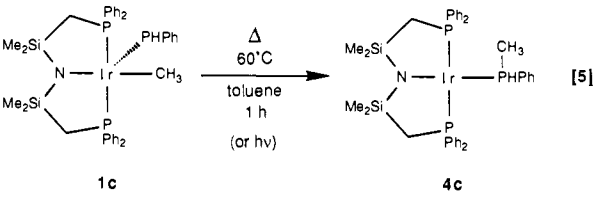

sponding cyclometalated phosphine derivative could not be detected with ^1H or $^{31}P\{^1H\}$ NMR spectroscopy. This same phosphine complex **4c** is produced upon photolysis of **1c** (140-W Hg lamp, 18 h, C_6D_6) as shown in eq 4.

Kinetic Studies. A number of kinetic studies were undertaken. First, the thermolytic conversion of $Ir(CH_3)PPh_2[N(SiMe_2CH_2PPh_2)_2]$ (**1a**) to *fac*-$Ir(\eta^2\text{-}CH_2PPh_2)H[N(SiMe_2CH_2PPh_2)_2]$ (**3a**) and of **3a** to $Ir(PMePh_2)[N(SiMe_2CH_2PPh_2)_2]$ (**4a**) were investigated. Second, the conversion of the phenylphosphide derivative $Ir(CH_3)PHPh[N(SiMe_2CH_2PPh_2)_2]$ (**1c**) directly to $Ir(PHMePh)[N(SiMe_2CH_2PPh_2)_2]$ (**4a**) was examined. This last transformation differs from the former as no corresponding cyclometalated intermediate could be detected; therefore these kinetic results are considered in a separate section.

(23) Appleton, T. G.; Clark, H. C.; Manzer, L. E. *Coord. Chem. Rev.* **1973**, *10*, 335.
(24) (a) Fryzuk, M. D.; MacNeil, P. A.; Rettig, S. J. *J. Am. Chem. Soc.* **1987**, *109*, 2803. (b) Fryzuk, M. D.; MacNeil, P. A.; Rettig, S. J. *Organometallics* **1985**, *4*, 1145.
(25) (a) Schmidbaur, H.; Blaschke, G. *Z. Naturforsch. B* **1980**, *35*, 584. (b) Werner, H.; Werner, R. J. *J. Organomet. Chem.* **1981**, *C60*, 209.

Table IV. Observed Rate Constants and Activation Parameters for the Conversion of $Ir(CH_3)PPh_2[N(SiMe_2CH_2PPh_2)_2]$ (**1a**) to fac-$Ir(\eta^2$-$CH_2PPh_2)H[N(SiMe_2CH_2PPh_2)_2]$ (**3a**)

temp, °C	10^3k_{obs}, s^{-1}	temp, °C	10^3k_{obs}, s^{-1}
In Toluene		In Hexanes	
73	0.54	60	0.06
83	0.84	67	0.14
97[a]	1.04	78	0.42
108	1.90	87	1.10
$\Delta H^\ddagger$ = 52 ± 15 kJ mol^{-1}		$\Delta H^\ddagger$ = 103 ± 20 kJ mol^{-1}	
$\Delta S^\ddagger$ = −163 ± 40 J K^{-1} mol^{-1}		$\Delta S^\ddagger$ = −16 ± 3 J K^{-1} mol^{-1}	

[a] The run at 97 °C was repeated, k_{obs} = 1.07 × 10^{-3} s^{-1}. Thus the uncertainty of 0.03 × 10^{-3} in the k_{obs} values was used to determine the error in the $\Delta H^\ddagger$ and $\Delta S^\ddagger$ values.

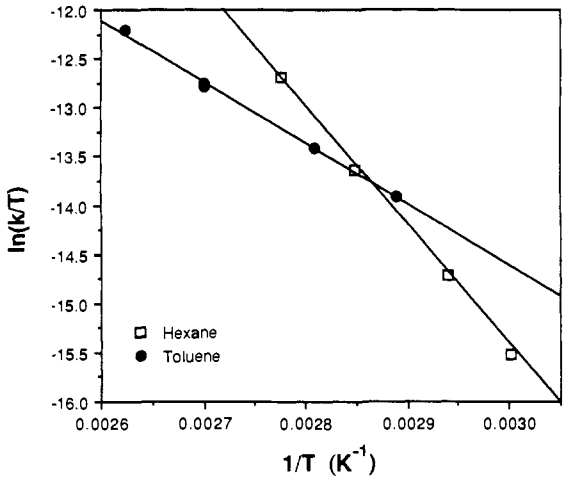

Figure 3. Eyring plot for the conversion of **1a** to **3a** in toluene and hexanes.

Because diphenylphosphide complex **1a** is colored (λ_{max} = 538 nm, ϵ = 2850 mol^{-1} L cm^{-1}), its rearrangement to **3a** (eq 2) in toluene was conveniently studied by following the decrease in the intensity of the band at 538 nm with time using UV–vis spectroscopy. Analysis of the spectral changes showed that the thermolysis rates were first order in the concentration of **1a** (data taken for at least 3 half-lives or more), as demonstrated by the linear plot of ln $(A_t - A_\infty)$ vs time. Measurements of the reaction rate were carried out at four different temperatures between 73 and 108 °C (Table IV). The plot of ln (k_{obs}/T) vs $1/T$ yielded a straight line (Figure 3), from which the following activation parameters were calculated: $\Delta H^\ddagger$ = 52 ± 15 kJ mol^{-1}, $\Delta S^\ddagger$ = −163 ± 40 J K^{-1} mol^{-1}. The $\Delta S^\ddagger$ value is a rather large negative number in toluene, larger than would be expected for a unimolecular process.[26] To test the influence of solvent, the thermolysis was also performed in hexanes; the activation parameters were found to be remarkably different: $\Delta H^\ddagger$ = 103 ± 20 kJ mol^{-1}, $\Delta S^\ddagger$ = −16 ± 3 J K^{-1} mol^{-1} (Table IV and Figure 3). The activation enthalpy is almost doubled in hexanes as compared to toluene, but this is now offset by a less negative activation entropy value; this suggests that the solvation effects contribute to the overall activation parameters. Thus in toluene, the large negative entropy of activation may be due to solvation of the phenyl rings of the diphenylphosphide unit and the phenyl substituents of the ancillary ligand in the transition state. Such solvation would give rise to substantial loss of translational degrees of freedom similar to that found in bimolecular reactions. The kinetic isotope effect (k_H/k_D) for this process was also determined; thermolysis of **1a**-CD_3 in hexanes at 67 °C was followed by UV–vis spectroscopy, and the k_H/k_D was found to be 1.6 ± 0.1, which indicates that C–H bond breaking is involved in the transition state.

(26) Benson, S. W. *Thermochemical Kinetics*; 2nd ed.; Wiley: Toronto, 1976; Chapter 2, p 78.

Table V. Observed Rate Constants and Activation Parameters for the Thermolytic Conversion of fac-$Ir(\eta^2$-$CH_2PPh_2)H[N(SiMe_2CH_2PPh_2)_2]$ (**3a**) to $Ir(PCH_3Ph)[N(SiMe_2CH_2PPh_2)_2]$ (**4a**) in Toluene

temp, °C	10^5k_{obs}, s^{-1}	temp, °C	10^5k_{obs}, s^{-1}
91[a]	0.87	102	2.31
94	1.03	112	6.59
$\Delta H^\ddagger$ = 107 ± 2 kJ mol^{-1}			
$\Delta S^\ddagger$ = −49 ± 6 J K^{-1} mol^{-1}			

[a] The run at 91 °C was repeated and k_{obs} = 0.94 × 10^{-5} s^{-1}. An error of 0.07 × 10^{-5} was used in all the k_{obs} values in calculating the errors in the activation parameters.

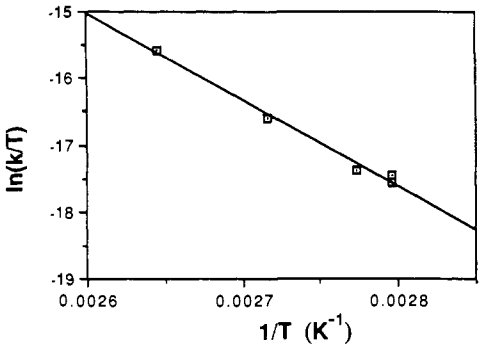

Figure 4. Eyring plot for the conversion of **3a** to **4a** in toluene.

Cyclometalated hydride complex fac-$Ir(\eta^2$-$CH_2PPh_2)H[N(SiMe_2CH_2PPh_2)_2]$ (**3a**) shows an absorption band at 360 nm (ϵ = 5425 mol^{-1} L cm^{-1}) in the UV–vis spectrum. Freshly prepared samples of **3a** were thermolyzed in toluene; the decrease in the absorption band at 360 nm was followed as **3a** converted to the corresponding phosphine complex, $Ir(PCH_3Ph_2)[N(SiMe_2CH_2PPh_2)_2]$ (**4a**) (eq 3). Again, the reaction was first order in the concentration of **3a** with k_{obs} = 6.59 × 10^{-5} s^{-1} at 112 °C. The transformation rates, determined at four temperatures in the range 91–112 °C, yielded the following activation parameters: $\Delta H^\ddagger$ = 107 ± 2 kJ mol^{-1} and $\Delta S^\ddagger$ = −49 ± 6 J K^{-1} mol^{-1} (Table V and Figure 4). The kinetic isotope effect was determined by heating the deuteride complex fac-$Ir(\eta^2$-$CD_2PPh_2)D[N(SiMe_2CH_2PPh_2)_2]$ (d_3-**3a**) at 112 °C in toluene. Comparison of the observed rate constants yielded k_H/k_D to be 1.6 ± 0.1 which coincidentally is the same as the k_H/k_D value observed for the thermolysis of **1a** to **3a** at 67 °C in hexanes. The influence of solvent was not investigated.

Mechanism of Carbon–Phosphorus Bond Formation. Two possible mechanisms for the aforementioned thermolysis transformations are shown in Scheme IV. In path A, the proposed first step involves α-hydride abstraction[27] by the phosphide group from the coordinated methyl ligand to generate the five-coordinate methylidene phosphine adduct $Ir(=CH_2)(PHR_2)[N(SiMe_2CH_2PPh_2)_2]$ (**6**). Oxidative addition (or α-elimination) of the phosphine P–H unit at the metal center produces the six-coordinate hydride phosphide intermediate **A**. This is followed by the migratory insertion of the phosphide ligand to the methylidene to yield the intermediate **B** having a dangling methylenephosphine moiety. These last two steps could also be reversed: first, migratory insertion of the methylidene to the *phosphine* generates a square-planar intermediate with a coordinated ylide, i.e., $Ir(^-CH_2P^+HPh_2)[N(SiMe_2CH_2PPh_2)_2]$, followed then by oxidative addition (or β-elimination) of the P–H moiety produces **B**. The lone pair on the uncoordinated phosphine of **B** can then bind to the coordinatively unsaturated iridium(III) center to generate species **3** (or **7**, vide infra). Further thermolysis of octahedral hydride complex **3** produces the square-planar iridi-

(27) (a) Crocker, C.; Empsall, H. D.; Errington, R. J.; Hyde, E. M.; McDonald, W. S.; Markam, R.; Norton, M. C.; Shaw, B. L. *J. Chem. Soc., Dalton Trans.* **1982**, 1217. (b) Ling, S. S.; Puddephatt, R. J. *J. Chem. Soc., Chem. Commun.* **1982**, 412.

Scheme IV

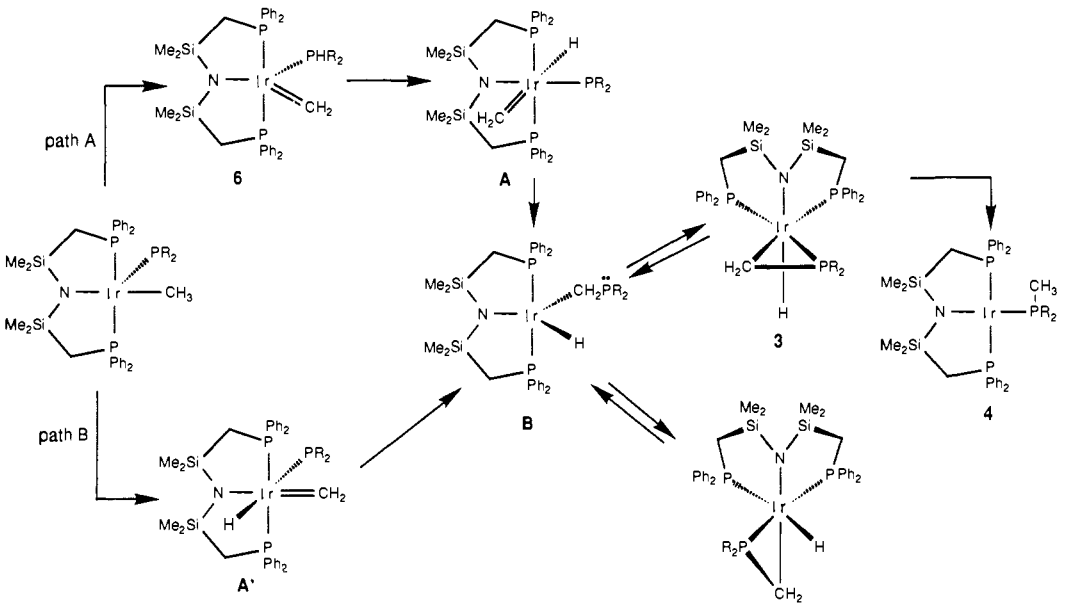

Scheme V

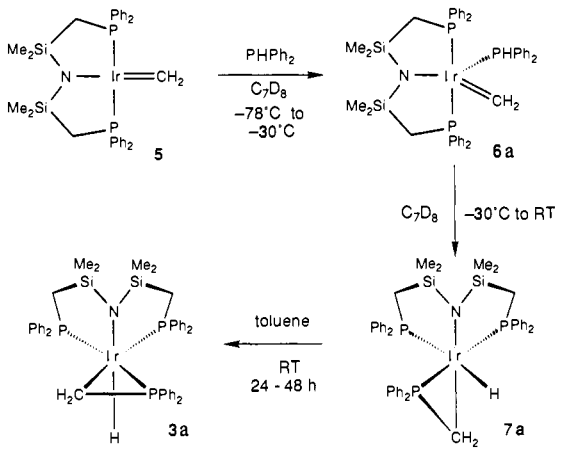

um(I) derivatives **4** via reductive elimination of the alkyl and hydride groups, and with ancillary ligand rearrangement.

An alternative mechanism is given as path B in Scheme IV. The first step is proposed to be α-elimination to the iridium center to form the hydride phosphide **A'** which is a stereoisomer of **A** in path A. Upon migratory insertion of the methylidene and the phosphide ligands the two paths converge since the identical postulated intermediate **B** is formed.

During the thermolytic transformation of **1a** to **3a** and **3a** to **4a**, none of the proposed intermediates in Scheme IV were observed by either ^1H or $^{31}P\{^1H\}$ NMR spectroscopy; however, the sequence of intermediates postulated in path A was supported via some independent experiments. The addition of 1 equiv of diphenylphosphine to a toluene solution of $Ir(=CH_2)[N(SiMe_2CH_2PPh_2)_2]$ (**5**)[28] at −78 °C caused the purple color of **5** to change to wine red (Scheme V). This color persisted up to −30 °C, above which it started to fade away to light yellow. The reaction was monitored by $^{31}P\{^1H\}$ and ^1H NMR spectroscopy. The complex formed at −78 °C was characterized as the diphenylphosphine adduct of methylidene complex $Ir(=CH_2)(PHPh_2)[N(SiMe_2CH_2PPh_2)_2]$ (**6a**). In the ^1H NMR spectrum, the methylidene protons in this complex are observed as a four-line pattern at +12.08 ppm ($^3J_{P,H}$ = 15 Hz) because of similar coupling to three phosphorus nuclei, whereas in the starting complex, a triplet at +16.44 ppm ($^3J_{P,H}$ = 14.4 Hz) is observed.[14] The silylmethyl protons are observed as two singlets, indicating inequivalent environments above and below the Ir–P–N–P plane. The P*H*Ph$_2$ proton would be expected to resonate as a doublet of triplets. One-half of this resonance was observed at 5.90 ppm but the other half was presumably obscured by the PPh_2 resonances. The $^{31}P\{^1H\}$ NMR spectrum obtained at −50 °C shows two singlets at 13.45 ppm (for the phosphorus nuclei belonging to the tridentate ligand) and 3.90 ppm (for the $PHPh_2$ ligand) in the integral ratio of 2:1. No coupling is observed between the coordinated diphenylphosphine and the tridentate ligand phosphine donors.

There are two other examples of iridium(I) methylidene complexes reported in the literature.[29] The complexes $Cp^*Ir(=CH_2)(PMe_3)$ and $Ir(=CH_2)(I)CO(PPh_3)_2$ have been prepared in situ at low temperatures only. The former complex decomposes above −40 °C, whereas the latter species yields an ylide complex at temperatures higher than −50 °C via intramolecular cyclometalation. With the hybrid tridentate ligand system, the trimethylphosphine adduct of the methylidene complex, $Ir(=CH_2)(PMe_3)[N(SiMe_2CH_2PPh_2)_2]$, was found to be stable only below 0 °C.[30] This species converted to $Ir(PMe_3)[N(SiMe_2CH_2PPh_2)_2]$ above 0 °C losing ethylene.

The solution of $Ir(=CH_2)(PHPh_2)[N(SiMe_2CH_2PPh_2)_2]$ (**6a**) when warmed above −30 °C, slowly rearranged to *fac*-$Ir(\eta^2\text{-}CH_2PPh_2)H[N(SiMe_2CH_2PPh_2)_2]$ (**7a**) in which the hydride ligand was trans to one of the phosphorus nuclei; this complex is a stereoisomer of the cyclometalated derivative **3a** obtained upon controlled thermolysis of the methyl phosphide **1a** (eq 2). The transformation of the phosphine adduct **6a** to **7a** was clean and no other species were detected during this process. The $^{31}P\{^1H\}$ NMR spectrum of **7a** consists of an AMX pattern indicating all three phosphorus nuclei are nonequivalent; in the corresponding ^1H NMR spectrum four singlets for the silylmethyl protons and four multiplets for the ligand backbone methylene protons are observed. One of the most informative features is the hydride resonance for **7a** which is observed as a doublet of doublet of doublets at −11.88 ppm (trans to a phosphorus nucleus) that shows a large trans coupling ($^2J_{P,H(trans)}$ = 133.3 Hz) to one of the phosphorus nuclei and cis couplings to the other two phosphorus centers ($^2J_{P,H(cis)}$ = 19.8 Hz, $^2J_{P,H(cis)}$ = 11.8 Hz). Complex **7a**

(28) Fryzuk, M. D.; MacNeil, P. A.; Rettig, S. J. *J. Am. Chem. Soc.* **1985**, *107*, 6708.

(29) (a) Klein, D. P.; Bergman, R. G. *J. Am. Chem. Soc.* **1989**, *111*, 3079. (b) Clark, G. R.; Roper, W. R.; Wright, A. H. *J. Organomet. Chem.* **1984**, *C17*, 273.

(30) Massey, R. L. M.Sc. Thesis, University of British Columbia, Vancouver, Canada, 1989.

Table VI. Observed Rate Constants and Activation Parameters for the Isomerization of **7a** to **3a** in Toluene

temp, °C	$10^4 k_{obs}$, s^{-1}	temp, °C	$10^4 k_{obs}$, s^{-1}
36	0.50	56	4.87
46	1.84	59	7.15

$\Delta H^{\ddagger} = 95 \pm 10$ kJ mol^{-1}

$\Delta S^{\ddagger} = -3 \pm 2$ J K^{-1} mol^{-1}

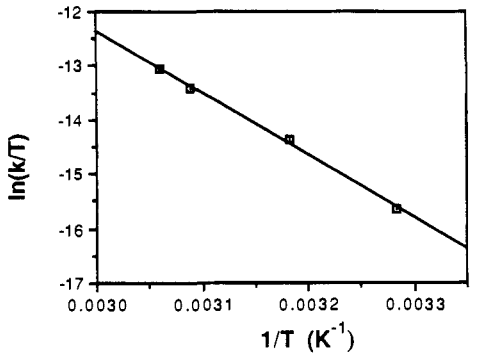

Figure 5. Eyring plot for the thermolytic conversion of **7a** to **3a** in toluene.

was stable in solution only for a few hours at room temperature, but it could be isolated as pale yellow crystals which were stable under an inert atmosphere at room temperture for long periods of time. Within 48 h in solution, however, **7a** completely isomerized to its stereoisomer **3a**, in which the hydride ligand was trans to the amide donor (Scheme V).

For the conversion of **7a** to **3a**, standard first-order kinetics were observed. The appearance of complex **3a** was followed by UV–vis spectroscopy at 360 nm. The observed rate constants at various temperatures (36–59 °C) are listed in Table VI. An Eyring plot of the data, ln (k/T) vs $1/T$ (Figure 5), yielded the activation enthalpy and entropy, $\Delta H^{\ddagger} = 95 \pm 10$ kJ mol^{-1}, $\Delta S^{\ddagger} = -3 \pm 2$ J K^{-1} mol^{-1}, respectively.

The five-coordinate iridium(III) hydride complex **B** is proposed (Scheme VI) as an intermediate in the isomerization of **7a** to **3a**. There exists indirect evidence for the involvement of **B** via a trapping experiment. Exposing the benzene solution of **7a** or **3a** to 1 atm of CO gas at room temperature for 48 h afforded a six-coordinate iridium(III) hydrido carbonyl species **8a** containing the η^1-CH_2PPh_2 ligand (Scheme VI). This complex was isolated as pale yellow crystals. The reaction of **7a** with CO gas was followed by UV–vis spectroscopy at 46 °C and the k_{obs} (1.82×10^{-4} s^{-1}) was found to be essentially identical with the k_{obs} value for the isomerization of **7a** to **3a** at this temperature (Table VI) and independent of CO pressure. This supports the proposal that the conversion of the kinetic isomer **7a** to the thermodynamic form **3a** requires dissociation of the cyclometalated phosphine and ancillary ligand rearrangement via an unobserved intermediate such as **B**.

The ^1H NMR spectrum of **8a** consists of two sharp singlets for the silyl methyl protons and two sets of doublets of virtual triplets for the $SiCH_2P$ protons of the ligand backbone, thus indicating trans disposition of the chelating phosphines. Most informative is the hydride region which is comprised of a triplet of doublets at −6.50 ppm ($^2J_{P,H} = 18.0$ Hz, $^3J_{P,H} = 9.0$ Hz). The $^2J_{H,C}$ coupling (54.0 Hz) observed in the ^1H NMR spectrum of the ^{13}CO-enriched complex helped to determine the trans disposition of the hydride and carbonyl ligands. In the $^{13}C\{^1H\}$ NMR spectrum, the ^{13}CO ligand is observed as a doublet of triplets at 179.88 ppm ($^2J_{P,C} = 11.0$ Hz, $^3J_{P,C} = 5.9$ Hz).[31]

Examples of transition-metal complexes containing the η^1-CH_2PR_2 ligand are rare.[32] The complex $CpRe(\eta^1\text{-}CH_2PMe_2)H(PMe_3)_2$ could be prepared only in situ at temperatures below 10 °C.[32b] At room temperature in benzene solution, it converted to $CpRe(Ph)H(PMe_3)_2$ via reductive elimination of trimethylphosphine and C–H activation of the solvent. Similarly, hydrido carbonyl species $Ir(\eta^1\text{-}CH_2PPh_2)H(CO)[N(SiMe_2CH_2PPh_2)_2]$ (**8a**) reductively eliminates methyldiphenylphosphine in solution (benzene) over a period of a week at room temperature and is converted to the previously reported iridium(I) carbonyl complex, $Ir(CO)[N(SiMe_2CH_2PPh_2)_2]$.[19]

Scheme VI

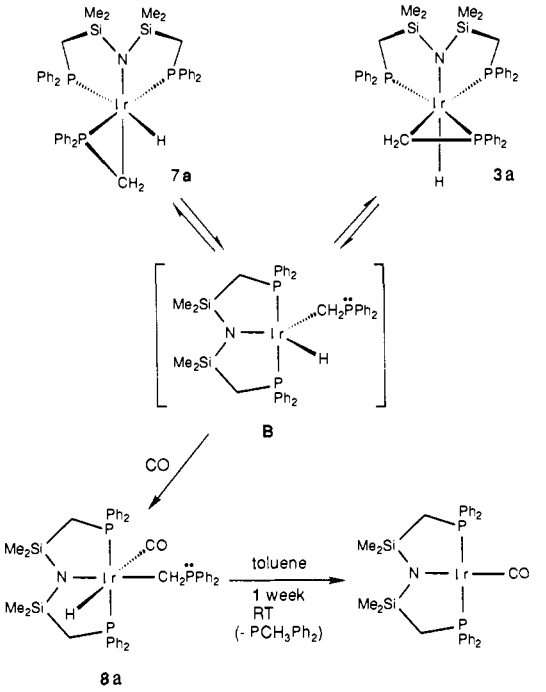

Another piece of evidence for the involvement of an intermediate similar to **B** in the formation of the metallacycle complexes **3** comes from the reaction of $LiCH_2PPh_2$·TMEDA with $Ir(CH_3)I[N(SiMe_2CH_2PPh_2)_2]$. The species $Ir(CH_3)(\eta^2\text{-}CH_2PPh_2)[N(SiMe_2CH_2PPh_2)_2]$ was produced, in which the tridentate ligand has facial geometry (as indicated by the ^1H and $^{31}P\{^1H\}$ NMR spectroscopy). The reaction presumably proceeds via a five-coordinate complex similar to **B** containing the η^1-CH_2PPh_2 ligand which undergoes ring closure to form the six-coordinate η^2-CH_2PPh_2 complex. However, the species $Ir(CH_3)(\eta^2\text{-}CH_2PPh_2)[N(SiMe_2CH_2PPh_2)_2]$ was found to be unstable in solution as it decomposed within a day.

Discussion of the Kinetic and Mechanistic Experiments. The thermal transformation of the square-pyramidal methyliridium phosphide complexes (**1**) to an isolable octahedral cyclometalated hydride intermediate (**2**) and finally on to square-planar Ir(I) complex (**4**) undoubtedly proceeds through a complex mechanism. Not only is there formation of a C–P bond accompanied by breaking and making of a C–H bond, but there is also ancillary ligand isomerization from quasimeridional (phosphine donors trans) to facial back to meridional. Simple first-order kinetics cannot generally be used to provide details on such a complicated mechanism, but in this case a number of straightforward proposals can be discussed.

In Scheme IV, it is not possible to exclude either path A or path B, but there is more supporting evidence for path A. For example, the ability to access the same products via formation of the phosphine adduct of the methylidene (cf. **6a**, Scheme IV) suggests

(31) (a) Deutsch, P. P.; Eisenberg, R. *Organometallics* **1990**, *9*, 709. (b) Mann, B. E.; Taylor, B. F. *^{13}C NMR Data for Organometallic Compounds*; Academic: New York, 1981.

(32) (a) Hester, D. M.; Yang, G. K. *Organometallics* **1991**, *10*, 369. (b) Blandy, C.; Locke, S. A.; Young, S. J.; Schore, N. E. *J. Am. Chem. Soc.* **1988**, *110*, 7540. (c) Wenzel, T. T.; Bergman, R. G. *J. Am. Chem. Soc.* **1986**, *108*, 4856. (d) Karsch, H. H.; Appelt, A. *Phosphorus Sulfur* **1983**, *18*, 287. (e) Engelhard, L. M.; Jacobsen, G. E.; Raston, C. L.; White, A. H. *J. Chem. Soc., Chem. Commun.* **1984**, 220. (f) Chiu, K. W.; Wong, W. K.; Wilkinson, G.; Galas, A. M. R.; Hursthouse, M. B. *Polyhedron* **1982**, *1*, 37.

that abstraction of the α-C–H by the lone pair on the phosphide is a viable route; more importantly, this is probably the rate-determining step in path A since methylidene phosphine **6a** could not be observed in the thermolysis of methyl phosphide complexes **1**. The large negative entropy of activation ($\Delta S^{\ddagger}$) is consistent with the formation of a highly-ordered four-centered transition state of the type shown in **C**; in this transition state, C–H bond making and bond breaking are occurring nonlinearly[33] and thus an isotope effect of 1.6 is reasonable.

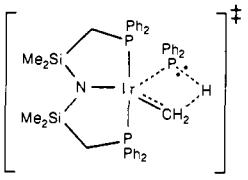

C

Such large and negative $\Delta S^{\ddagger}$ values are characteristic of four-centered transition states proposed for cyclometalation reactions;[34] for example, the alkoxide complex $Zr(OAr')_2(CH_2Ph)_2$, where OAr' = 2,6-di-*tert*-butylphenoxide, undergoes intramolecular activation of one of the C–H bonds of the *tert*-butyl groups when heated in toluene and affords the corresponding cyclometalated complex $Zr(OC_6H_3{}^tBuCMe_2CH_2)(OAr')(CH_2Ph)$ with elimination of 1 equiv of toluene. Kinetic measurements of the cyclometalation step showed the reaction to be unimolecular with the following activation parameters: $\Delta H^{\ddagger}$ = 90 kJ mol^{-1}, $\Delta S^{\ddagger}$ = −80 J K^{-} mol^{-1}.[35]

Although not observable under the thermolysis conditions, the next isolable species in the proposed mechanism is **7a**, obtained from the low-temperature addition of $HPPh_2$ to the methylidene (Scheme V). Upon further thermolysis **7a** isomerizes to the more stable stereoisomer **3a**; the isomerization occurs withg $\Delta G^{\ddagger} \approx \Delta H^{\ddagger}$ = 95 ± 10 kJ mol^{-1} as $\Delta S^{\ddagger}$ is essentially negligible. In addition, the rate of the reaction of **7a** with CO generates the same k_{obs} as measured for the thermolysis reaction consistent with the rate-determining step being phosphine dissociation; a transition state similar to **D** below with the cyclometalated phosphine slightly dissociated is reasonable and suggests that ancillary ligand rearrangement from facial to meridional occurs subsequent to the rate-determining dissociation step.

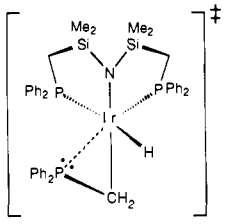

D

The rearrangement of the thermodynamic isomer **3a** to the square-planar iridium(I) complex **4a** occurs with $\Delta H^{\ddagger}$ = 107 ± 2 kJ mol^{-1} and $\Delta S^{\ddagger}$ = −49 ± 6 J mol^{-1} K^{-1}; in addition, a primary kinetic isotope effect of 1.6 ± 0.1 was found. A rather speculative transition state **E** is shown below in which a highly-ordered, three-centered Ir–C–H interaction rationalizes the negative $\Delta S^{\ddagger}$ and the isotope effect. Such a transition state obviates the formation of a transient σ-complex, normally invoked for reductive elimination of alkyl hydride complexes,[36] since the phosphine donor is already bound to the iridium. The formation of the five-coordinate intermediate **B** (Scheme VI) is not consistent with the measured kinetic parameters. It should be noted that **B** can be formed from **3a** as evidenced by the reaction with CO to produce **8a** as shown in Scheme VI. However, it must be concluded that reductive elimination via B to form iridium(I) complex **8a** is not part of the rate-determining step.

(33) March, J. *Advanced Organic Chemistry*, 2nd ed.; McGraw-Hill: Toronto, 1977; p 205.
(34) Rothwell, I. P. *Polyhedron* **1985**, *4*, 177.
(35) Latesky, S. L.; McMullen, A. K.; Rothwell, I. P.; Huffmann, J. C. *J. Am. Chem. Soc.* **1985**, *107*, 5981.
(36) Parkin, G.; Bercaw, J. E. *Organometallics* **1989**, *8*, 1172.

Table VII. Observed Rate Constants and Activation Parameters for the Thermolytic Conversion of $Ir(CH_3)PHPh[N(SiMe_2CH_2PPh_2)_2]$ (**1c**) to $Ir(PHCH_3Ph)[N(SiMe_2CH_2PPh_2)_2]$ (**4c**)

temp, °C	$10^3 k_{obs}$, s^{-1}	temp, °C	$10^3 k_{obs}$, s^{-1}
In Toluene		In Hexanes	
69	0.430	54[a]	0.176
82	1.600	65	0.476
86	2.102	74	1.008
93	2.800	79	1.327
$\Delta H^{\ddagger}$ = 82 ± 10 kJ mol^{-1}		$\Delta H^{\ddagger}$ = 77 ± 8 kJ mol^{-1}	
$\Delta S^{\ddagger}$ = −71 ± 20 J K^{-1} mol^{-1}		$\Delta S^{\ddagger}$ = −83 ± 8 J K^{-1} mol^{-1}	

[a] The run at 54 °C was repeated and k_{obs} = 0.178 × 10^{-3} s^{-1}. Therefore, an error of 0.002 × 10^{-3} in the k_{obs} values was used to calculate the uncertainty in the activation parameters.

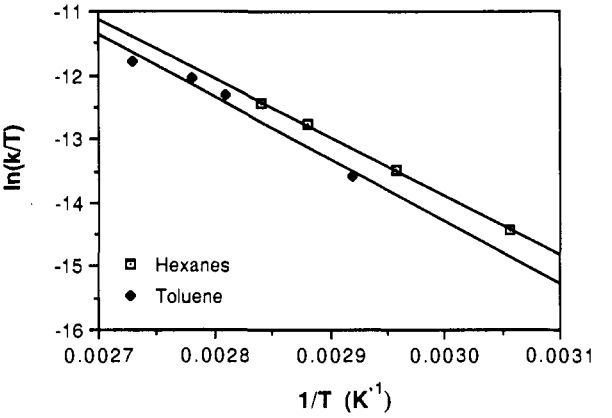

Figure 6. Eyring plot for the thermolysis of **1c** to **4c** in toluene and hexanes.

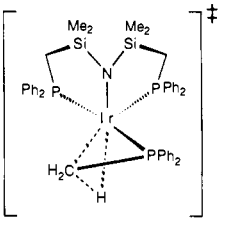

E

Kinetics of Phenylphosphide Complex 1c Rearrangement. Thermolysis of phenylphosphide complex $Ir(CH_3)PHPh[N(SiMe_2CH_2PPh_2)_2]$ (**1c**) to iridium(I) derivative $Ir(PHPhMe)[N(SiMe_2CH_2PPh_2)_2]$ (**4c**) was followed by UV–vis spectrophotometry because the starting material **1c** is colored (λ_{max} = 462 nm, ϵ = 1820 mol^{-1} L cm^{-1}). First-order kinetics were observed for this conversion; rates were determined at four temperatures in toluene in the range of 69–93 °C (Table VII). The activation parameters, $\Delta H^{\ddagger}$ and $\Delta S^{\ddagger}$, are 82 ± 10 kJ mol^{-1} and −71 ± 7 J K^{-1} mol^{-1}, respectively (Figure 6, Table VII). Thermolysis of the phenylphosphide complex was also followed in hexanes (λ = 515 nm, ϵ = 1951 mol^{-1} L cm^{-1}), and the activation parameters ($\Delta H^{\ddagger}$ = 77 ± 8 kJ mol^{-1}, $\Delta S^{\ddagger}$ = −83 ± 8 J K^{-1} mol^{-1}) obtained were similar to those obtained in toluene (Figure 6, Table VII). Any specific involvement of the solvent in the transition state is therefore precluded. No primary kinetic isotope effect was observed for this transformation with use of $Ir(CD_3)PHPh[N(SiMe_2CH_2PPh_2)_2]$ (k_H/k_D = 1.0 ± 0.1 at 74 °C in hexanes), thus indicating that no carbon–hydrogen bond breaking is involved in the transition state.

Mechanistic Considerations. It is proposed that the thermolysis of phenylphosphide complex **1c** proceeds through a different mechanism than that discussed above for diphenylphosphide derivative **1a** (Scheme IV). This is based on the following three differences in the experimental results of the thermolysis of **1c**:

(i) no observation of a cyclometalated intermediate similar to **3**; (ii) the lack of a solvent effect in the thermolysis, and (iii) a negligible kinetic isotope effect. The lack of a primary kinetic isotope effect implies that C–H bond making or breaking is not involved in the rate-determining step. One straightforward proposal is that the mechanism for this transformation proceeds via a simple reductive coupling of the phosphide unit and the methyl ligand.[37] A transition state similar to **F** below would be appropriate since it has a highly-ordered, three-centered interaction with no C–H cleavage involved.

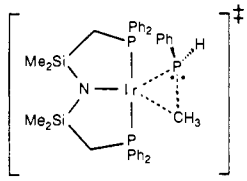

F

The fact that an intermediate cyclometalated hydride species is not detected in the thermolysis can be because either it is too reactive to be observed by NMR spectroscopy or it does not form at all during the thermolysis process; the latter proposal is consistent with the above transition state **F**. To test the former possibility, a separate experiment involving the reaction of PH_2Ph with methylidene complex $Ir(=CH_2)[N(SiMe_2CH_2PPh_2)_2]$ (**5**) was conducted in an attempt to access the cyclometalated hydride species in analogy to Scheme V. The reaction proceeded instantaneously at −78 °C as the purple color of the methylidene complex **5** changed to light yellow; this new derivative was characterized as *fac*-$Ir(\eta^2\text{-}CH_2PHPhH[N(SiMe_2CH_2PPh_2)_2]$ (**7c**) by ^1H and $^{31}P\{^1H\}$ NMR spectroscopy (eq 6). Interestingly, the phosphine adduct of methylidene complex $Ir(=CH_2)(PH_2Ph)[N(SiMe_2CH_2PPh_2)_2]$ (**6c**) was not detected even at low temperatures. The ^1H NMR spectrum indicates that the hydride

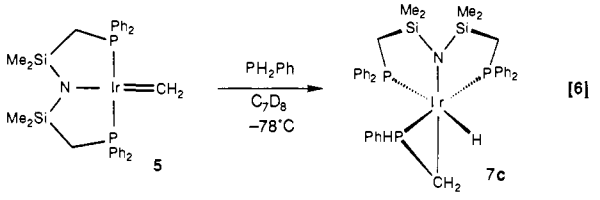

5 **7c** [6]

ligand in **7c** is trans to a phosphine donor of the tridentate ligand (−12.87 ppm, dt, $^2J_{P,H(trans)}$ = 149.3 Hz, $^2J_{P,H(cis)}$ = 19.1 Hz). The geometry at the chiral phosphorus in η^2-CH_2PHPh ligand could not be ascertained from the NMR data; however, only one diastereomer was apparently found. This complex in solution does not isomerize to the analogous, isomeric cyclometalated derivative in which the hydride ligand is trans to the amide moiety, and neither does it convert to the square-planar iridium(I) complex, $Ir(PHPhMe)[N(SiMe_2CH_2PPh_2)_2]$ (**4c**). Heating the toluene solution of **7c** at 80 °C for 30 min resulted in complete decomposition. Although by no means conclusive, this supports the proposal that a different mechanism is operative.

Why is there a difference in mechanism upon going from diphenylphosphide complex **1a** to phenylphosphide complex **1c**? The difference is not due to the higher basicity[38] of the phenylphosphide ligand as compared to the diphenylphosphide moiety, because even the very basic dimethylphosphide complex **1b** rearranges via the corresponding cyclometalated derivative **3b**; although no kinetic studies were performed on the dimethylphosphide system, it is assumed that a similar mechanism to the diphenylphosphide

Scheme VII

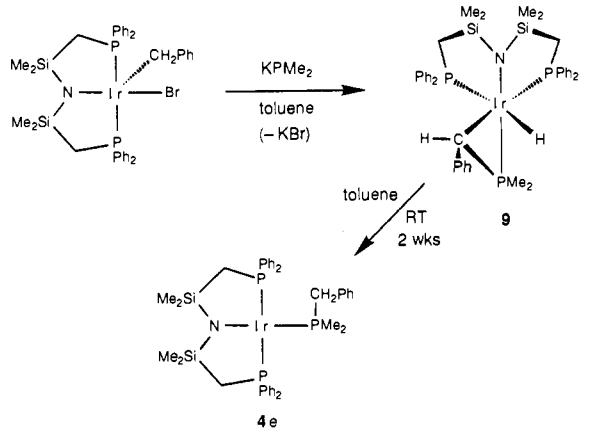

(37) A more complex proposal is that the phosphide spontaneously α-eliminates to generate a phosphinidene species of the formula $Ir(=PPh)(CH_3)H[N(SiMe_2CH_2PPh_2)_2]$ which then undergoes migratory insertion with the methyl ligand to generate the methylphenylphosphide–hydride complex $Ir(PMePh)H[N(SiMe_2CH_2PPh_2)_2]$; subsequent reductive elimination of the hydride and the phosphide generates the phosphine derivative. No direct mechanistic studies were performed to preclude this proposal.

(38) Kosolapoff, G. M. *Organophosphorus Compounds*; John Wiley: New York, 1950; Chapter 1, p 24.

complex obtains. However, the different reactivities can be rationalized in terms of the transition states. A four-centered transition state (labelled **C**) might be necessary in the diphenylphosphide complex because of steric strain which only allows access to the C–H bond of the methyl ligand. For the less sterically encumbered phenylphosphide complex, the three-centered transition state **F** above, where direct C–P bond formation occurs, is possible.

This change in mechanism upon varying the substituent at the phosphide ligand also adds credence to the suggestion that, in the mechanism outlined in Scheme IV, path A is more appropriate than path B. Were path B operative the rate-determining step (α-elimination to the metal) should not be sensitive to a change in substituent at phosphorus.

Miscellaneous Reactions. In earlier work,[6] we reported that there were limitations in the preparation of phosphide alkyl derivatives of iridium by the method shown in eq 1, limitations that were primarily steric in origin. For example, attempts to prepare phosphide complexes with other than a methyl ligand bound to the iridium failed. Even the reaction of $LiPMe_2$ with benzyliridium complex $Ir(CH_2Ph)Br[N(SiMe_2CH_2PPh_2)_2]$ gave no reaction even after 1 week, just recovery of starting materials. However, the reaction of the *potassium* salt, $KPMe_2$, with this benzyliridium derivative does proceed, but not to generate the expected phosphide complex. Instead, the cyclometalated complex *fac*-$Ir\{\eta^2\text{-}CHPhPMe_2)[N(SiMe_2CH_2PPh_2)_2]$ (**9**) was isolated in good yield (80%) as shown in Scheme VII. The stereochemistry at the metal center of this octahedral complex was easily established by ^1H and $^{31}P\{^1H\}$ NMR spectroscopy as being that stereoisomer with the hydride ligand trans to one of the ancillary phosphine ligands and all three phosphorus donors cis disposed on the complex; it should be noted that this stereoisomer is distinct from both of the already mentioned octahedral cyclometalated type hydride complexes. Because complex **9** itself is chiral, the addition of a second stereogenic center at the benzylic carbon should generate diastereomers; as only one diastereomer was observed, it must be concluded that this reaction is completely stereoselective. The relative stereochemistry at the chiral benzylic carbon was not established, but the indicated diastereoisomer is assumed on simple steric grounds: the phenyl substituent on the benzylic carbon should point away from the phenyl substituents on the ancillary ligand. Presumably, phosphide complex $Ir(CH_2Ph)PMe_2[N(SiMe_2CH_2PPh_2)_2]$ (**1d**) forms but it was not detected. In solution the cyclometalated derivative **9** rearranges to generate iridium(I) complex $Ir(PMe_2CH_2Ph)[N(SiMe_2CH_2PPh_2)_2]$ (**4e**); however, in contrast to the reactions mentioned above, no hydride intermediates analogous to the other stereoisomeric cyclometalated complexes were detected.

Phenyliridium complex $Ir(Ph)I[N(SiMe_2CH_2PPh_2)_2]$ does not react with $LiPPh_2$, but upon reaction with $LiPMe_2$ iridium(I) phosphine complex $Ir(PMe_2Ph)[N(SiMe_2Ch_2PPh_2)_2]$ (**4f**) was obtained directly; no intermediates were observed.

Methyliridium iodide derivative $Ir(CH_3)I[N(SiMe_2CH_2PPh_2)_2]$ does not react with either $LiPBu^t_2$ or $KPBu^t_2$ even at 80 °C.

Scheme VIII

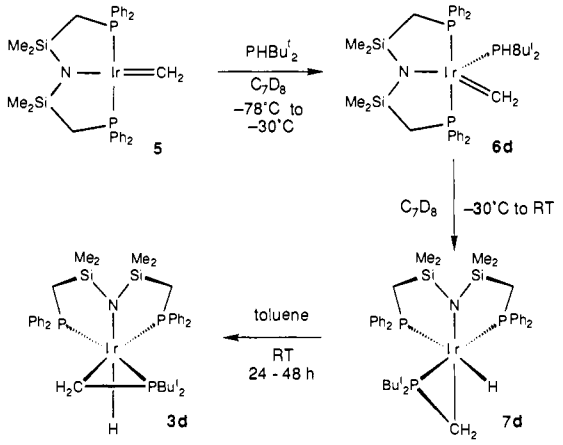

However, addition of di-*tert*-butylphosphine ($HPBu^t_2$) to methylidene complex **5** at −78 °C affords phosphine adduct $Ir(=CH_2)(PHBu^t_2)[N(SiMe_2CH_2PPh_2)_2]$ (**6d**), which, above −30 °C, rearranges to cyclometalated derivative **7d**. The stereochemistry was shown to be that analogous to the kinetic stereoisomer found for the diphenylphosphine series in which the hydride is trans to one of the phosphine donors of the ancillary ligand; further rearrangement occurs in solution to generate stereoisomer **3d** having the hydride trans to the amide donor. This is summarized in Scheme VIII.

Conclusions

A series of alkyl phosphide complexes of iridium(III) have been shown to rearrange both thermally and photochemically to ultimately generate iridium(I) phosphine complexes. For phenylphosphide derivative **1c** this process occurs with no detectable isotope effect (k_H/k_D = 1.0 (1)), thus indicating that breaking the C–H bond of the methyl ligand is probably not involved in the rate-determining step. It is proposed that the mechanism involves the direct reductive transfer of the methyl to the phosphide to generate iridium(I) phosphine complex $Ir(PHPhMe)[N(SiMe_2CH_2PPh_2)_2]$ (**4c**) via a three-centered transition state (cf. **F**).

With diphenyl- and dimethylphosphide derivatives **1a** and **1b**, the thermal rearrangement has been shown to involve the formation of cyclometalated hydride complexes *fac*-$Ir(\eta^2\text{-}CH_2PR_2)H[N(SiMe_2CH_2PPh_2)_2]$ as the kinetic products on the way to the formation of iridium(I) phosphine derivatives. Mechanistic studies on this transformation revealed that the rearrangement to the cyclometalated complexes is solvent dependent and involves a modest isotope effect (k_H/k_D = 1.6 (1)). Modelling studies using methylidene complex **5** provided strong evidence that the phosphide abstracts a C–H bond from the coordinated methyl via a highly solvated four-centered transition state (cf. **C**).

The formation of a cyclometalated hydride complex as a kinetic product on the way to the formation of a phosphine derivative is in complete contrast to literature precedent. Previous work[9] has shown that coordinatively unsaturated phosphine complexes can rearrange to cyclometalated derivatives via intramolecular C–H bond activation. In our system this is certainly not occurring. Presumably, the stability of square-planar iridium(I) phosphine complexes **4** is such that there is no tendency to undergo intramolecular C–H activation. Yet not all square-planar iridium(I) derivatives exhibit such stability,[39] and this therefore underscores the importance of ancillary ligands in determining the outcome of reactions within the coordination sphere of a particular metal complex.

Acknowledgment. We gratefully acknowledge NSERC of Canada for financial support in the form of operating grants and an E. W. R. Steacie Fellowship to M. D. F. Johnson-Matthey is also acknowledged for the generous loan of $IrCl_3$.

Supplementary Material Available: Tables of final atomic coordinates and thermal parameters for $Ir(CH_3)PPh_2[N(SiMe_2CH_2PPh_2)_2]$ (**1a**) and *fac*-$Ir(\eta^2\text{-}CH_2PPh_2)H[N(SiMe_2CH_2PPh_2)_2]$ (**3a**) (4 pages). Ordering information is given on any current masthead page.

(39) (a) Bennet, M. A.; Milner, D. L. *J. Am. Chem. Soc.* **1969**, *91*, 6983. (b) Tulip, T. H.; Thorn, D. L. *J. Am. Chem. Soc.* **1981**, *103*, 2448.

Synthesis and Structural Characterization of (η^4-Cyclopentadienone)(η^5-cyclopentadienyl)dicarbonylmolybdenum Hexafluorophosphate. A Template for the Stereospecific Construction of *cis*-4,5-Disubstituted-2-cyclopentenones

Lanny S. Liebeskind* and Agnès Bombrun

Contribution from the Department of Chemistry, Emory University, Atlanta, Georgia 30322.
Received May 17, 1991

Abstract: A stable, cationic metal π-complex of cyclopentadienone, (η^4-cyclopentadienone)(η^5-cyclopentadienyl)dicarbonylmolybdenum hexafluorophosphate, has been prepared in good yield. A variety of nucleophiles (RLi, RMgX, $NaCH(CO_2Et)_2$, $RCOCH_2Li$, enamine) add α to the cyclopentadienone C=O moiety and anti to the $CpMo(CO)_2$ group to give good yields of stable π-cyclopentenoyl products. These compounds have been demetalated by (1) protonation with CF_3COOH to give 5-substituted-2-cyclopentenones and (2) oxidation with $IOCOCF_3$ to give *cis*-5-substituted-4-(trifluoroacetoxy)-2-cyclopentenones. The cyclopentenoyl complexes derived from ketone enolate addition to the cyclopentadienone undergo intramolecular nucleophilic attack by the carbonyl oxygen giving the 2-oxabicyclo[3.3.0]-3,7-octadien-6-one ring system.

Introduction

The development of stereocontrolled methods for the construction of cyclopentanone-based ring systems remains an important goal in synthetic organic methodology.[1-4] Within this context, substituents are often attached at the 2- and 3-position on the cyclopent*anone* ring in a trans relative relationship via a

(1) Ellison, R. A. *Synthesis* **1973**, 397.

0002-7863/91/1513-8736$02.50/0